Canadian Journal of
Fisheries and
Aquatic Sciences

OPEN ACCESS | Research Article

Temperature, maximum size, and the Atlantic surfclam *Spisula solidissima*: the sensitivity of demographics to climate warming, the perfidy of food, and a vignette on size-limited management in bivalve fisheries

Eric N. Powell[a], **Autumn L. Moya**[a], **Daphne M. Munroe**[b], **Roger Mann**[c], **Sarah Borsetti**[b], **and Kelsey M. Kuykendall**[a]

[a]University of Southern Mississippi, Gulf Coast Research Laboratory, 703 East Beach Dr., Ocean Springs, MS 39564, USA; [b]Rutgers the State University of New Jersey, Haskin Shellfish Research Laboratory, 6959 Miller Ave, Port Norris, NJ 08349, USA; [c]Virginia Institute of Marine Science, William & Mary, 1370 Greate Rd., Gloucester Point, VA 23062, USA

Corresponding authors: **Eric N. Powell** (email: eric.n.powell@usm.edu); **Daphne M. Munroe** (email: dmunroe@hsrl.rutgers.edu)

Abstract

A dominant theme explaining intraspecific latitudinal size gradients is the temperature–size rule which states that growth rates decline but maximum sizes increase with declining temperatures over a species' range. Herein, the demographics of the Atlantic surfclam *Spisula solidissima* are evaluated relative to the temperature–size rule, followed by contemplations on the impact of climate change on its management. Analysis of latitudinal trends in size–frequency identifies the anticipated trend of increasing maximum size with decreasing temperature. A metabolic energetics model shows that variations in size accrue from the physiological impact of geographic variations in temperature modulated by variations in food supply. Lifetime fecundity declines with increasing temperature. Implications include the decline in maximum size towards the south limiting the southern stock as a larval source. As temperature increases, the more rapid early growth rate does not counterweigh the cap on size imposed by temperature. Thus, higher temperatures rob the species of reproductive potential. Management measures based on the size frequency are discussed, and specifically regulatory size limits on landings are identified as incompatible with the temperature–size rule.

Impact statement:

The contribution directly addresses the influence of climate change on the fisheries management of the Atlantic surfclam, with specific reference to size-limit regulations. This paper, more broadly, examines the influence of rising temperatures on the growth of Atlantic surfclams and, by extension, most of the Bivalvia.

Key words: temperature–size rule, Atlantic surfclam, maximum size, von Bertalanffy growth model, size-limit, fisheries management, climate change

Introduction

A continuing theme in rationalizing observed changes in size and morphology over geographically significant distances is the influence of temperature on morphological characteristics expressing some measure of size. Classic morphological-biogeographic rules, including Bergmann's rule which states that within a taxonomic clade, species of larger size are found in colder environments (e.g., Bergmann 1847; John 1933; Ray 1960; James 1970; McQueen et al. 2022), and Allen's rule, which states that animals adapted to colder climes have shorter and thicker limbs (Allen 1877; Ray 1960; McQueen et al. 2022), invoke temperature as the primary environmental effector influencing important morphological characteristics of species over latitudinal extents. A more general relationship between temperature and size in ectotherms has received considerable attention as it applies within species, with the general outcome that higher temperatures invoke as a morphological response smaller maximum size (Atkinson 1994). Thus, taking the latitudinal gradient as a prime example, larger individuals of a species will be found most likely at higher latitudes (DuBose et al. 2022; Männer et al. 2022). The relationship is well-described for a wide range of ectotherms, terrestrial, freshwater, and marine (e.g., Atkinson 1994; Forster et al. 2012; Irie et al. 2013; Pauly et al. 2022; Zang et al. 2023; Queiros et al. 2024). Whereas a range of specific explanatory hypotheses has been proffered (Atkinson 1994), the majority involve the confluence of physiological determinants allometrically scaling differentially with a measure of size, most often as a product of one process scaling with surface area and another with volume (Forster and Hirst 2012; Zuo et al. 2012; Verberk et al. 2021; Audzijonyte et al. 2022; Pauly et al. 2022). Gray (1928), in comparing salmon embryo size relative to egg size at different temperatures, documents possibly the earliest marine example that nonetheless exemplifies the widespread influence of temperature as it influences development and physiology through the surface area-to-volume ratio.

Although bivalve molluscs do not appear to follow Bergmann's rule (Nicol 1978; Berke et al. 2013; see Nowrot et al. 2017 for a regional exception), they are an interesting subset of the many taxa expressing predictable trends between size and temperature (Nicol 1964; Bauer 1992; Hochwald 2001; Männer et al. 2022), and indeed even over evolutionary time (Moss et al. 2016), as they demonstrate a classic relationship between the differential scaling of the processes determining growth and tissue maintenance. This relationship is primarily determined by the differential scaling of ingestion and respiration, reminiscent of arguments originally trumpeted by von Bertalanffy (1938), though clearly presaged by Pütter (1920), and expanded upon by many others (e.g., Jensen 1997; Ohnishi et al. 2012; Montalto et al. 2015). Not surprisingly, a growth model developed therefrom can be applied successfully to nearly every bivalve species, only the ocean quahog *Arctica islandica* being clearly divergent (Klinck et al. 2023). The scaling relationship of import is the classic surface area-to-volume relationship (Martinez del Rio and Karasov 2010), which, in the case of bivalves, is defined by the difference between the surface area of the food collection organ, the gill, an allometric scaling factor relative to length of ∼2, and the volume of the body tissue supporting respiration, an allometric relationship scaling with length of ∼3 (van der Veer et al. 2006). Even in species diverging from this generality, the higher scaling exponent for respiration persists (Le et al. 2017). This differential underpins nearly every metabolically based population dynamics model for bivalves (e.g., Powell et al. 1992; Ren and Ross 2005; Hofmann et al. 2006; van der Veer et al. 2006; Flye-Sainte-Marie et al. 2007; Freitas et al. 2009; Munroe et al. 2013*a*; Mangano et al. 2020; Zang et al. 2022) and undergirds most growth curves determined for bivalves, the majority of which approximate the von Bertalanffy relationship (e.g., Vakily 1992; Mancera and Mendo 1996; Smith et al. 1997; Hart and Chute 2009; Kilada et al. 2009; Selin 2010; Serna-Gallo et al. 2014; Mugabe et al. 2019).

The Atlantic surfclam, *Spisula solidissima*, is among the largest nonsymbiont-containing bivalves and notable as to the extensiveness of its geographic range, its biomass dominance, and its sensitivity to warming temperatures. *Spisula solidissima* is a cool temperate species, characteristic of the Virginian province (Hale 2010), and ranges from near Cape Hatteras along the U.S. east coast to Georges Bank and inshore into the southern portion of the Gulf of Maine, residing in regions with summer bottom-water temperatures that range between approximately 11 and 20 °C (Hofmann et al. 2018). Consequently, the species resides between the warmer inshore waters along the southern Mid-Atlantic Bight and the inshore boundary of the Cold Pool, a body of cold water occupying the central to outer continental shelf from Georges Bank, along the southern New England and Long Island coast, and downcoast from New Jersey to Virginia (Chen et al. 2018; Friedland et al. 2022), the inshore boundary of which partitions the cool temperate and boreal faunas (Powell et al. 2020*a*; Stromp et al. 2023). Within this region, *S. solidissima* is an archetypical benthic biomass dominant. One consequence is that this species supports one of the largest shellfish fisheries in the U.S. (McCay et al. 2011; Hofmann et al. 2018; Scheld et al. 2022).

Notably, the geographic domain in which this species resides has developed some notoriety due to the rapid warming of the Northwestern Atlantic relative to other parts of the world's oceans (Pershing et al. 2015; Saba et al. 2016; Friedland et al. 2020; Kessler et al. 2022; du Pontavice et al. 2023). The narrow upper thermal limit well-described for this species (Narváez et al. 2015; Spencer et al. in press) results in rapid physiological stress leading to starvation and death with persistent temperatures above ∼21 °C (e.g., Kim and Powell 2004; Narváez et al. 2015). The narrow upper thermal limit conspires with these warming temperatures to produce a species recognized as a bellwether of climate change in this region, with well-documented and surprisingly rapid, for a sedentary species, shifts in range offshore and north following the cool temperate water (Weinberg 2005; Hofmann et al. 2018; Timbs et al. 2019; Powell et al. 2020*b*; Stromp et al. 2023).

Spisula solidissima is noteworthy for the wide range of maximum sizes (typically estimated by the von Bertalanffy parameter L); size varies latitudinally (Chute et al. 2016; Munroe et al. 2016; Diaz et al. 2024) and onshore–offshore (Powell et al. 2020*b*; Stromp et al. 2023). Onshore–offshore trends in size may, in part, be due to recent settlement leading to a dominance of young animals offshore as ocean warming continues (e.g., Powell et al. 2020*b*), although an offshore limitation in food supply cannot be discounted as an abetting process (Marzec et al. 2010). The latitudinal effect, however, is not so easily explained. An alternative, the expression in this species of the temperature–size rule, is investigated herein as a likely explanation. The temperature–size relationship has not been modeled overtly and not well documented in bivalves, although much evidence suggests that such a relationship exists and may be a primary determinant of geographic trends in size. The physiology of *S. solidissima*, as modeled by Munroe et al. (2013*a*), Narváez et al. (2015), and Pousse et al. (2021), would be consistent with the invocation of the temperature–size rule as an explanation of the latitudinal trend in size, based on the variable scaling of ingestion and respiration in the species' metabolic energetics. Chintala and Grassle (2001) convey the potential for a temperature effect on size for *S. solidissima* (see also Savage 1976).

In this contribution, *S. solidissima* is first posed as a prototypical bivalve permitting evaluation of the degree to which the temperature–size rule is applicable to bivalves. Subsequently, again using *S. solidissima* as a prototypical case, a question is raised as to the implications of this physiological constraint on bivalve population dynamics across geographic regions from the standpoint of such important aspects of population dynamics as growth rate and fecundity relative to location within the temperature range conducing habitation in the benthic community. In doing so, the study builds upon a substantial literature within the Bivalvia relating growth rate and maximum size to other individual and population-level metrics such as growth efficiency (e.g., Allen 1971; Ohnishi et al. 2012), mortality rate (Brey and Gage 1997; Andrews and Mangel 2012; Then et al. 2015), and geographic distribution (Roy et al. 2001; Chute et al. 2016).

The *Spisula solidissima* temperature–size model

The model utilized to evaluate an expected relationship of maximum size, as typically defined by the von Bertalanffy parameter L , with temperature is based on the population dynamics models for *S. solidissima* specified by Munroe et al. (2013*a*) and Narváez et al. (2015) and specifically the equations listed in table 1 in Munroe et al. (2013*a*) and Narváez et al. (2015), which will not be represented here. Specifications leading to the estimation of assimilated energy and the proportion expended as respiration are each temperature dependent. The length–weight relationship is taken from Marzec et al. (2010), who report a number of parameter values also from Fay et al. (1983), Weinberg (2005), and NEFSC (2007), all of which are very similar. Temperature-dependent respiration rate is specified using a Q_{10} relationship with the base respiration rate adapted from Powell and Stanton (1985). Base filtration rate is obtained from Powell et al. (1992) with the temperature dependency adapted from Hofmann et al. (2006) and further specified to fit observations for *S. solidissima* as described in Munroe et al. (2013*a*). Of importance, the final influence of temperature on filtration rate follows a left-skewed parabola, typical of a physiology with a transient event margin characterized by temperatures above optimum producing physiological processes that persistently slow as temperature rises (Woodin et al. 2013; see also Talevi et al. 2023; Wagner et al. 2023), something Getz (2011) termed deficit stress. The result of the temperature dependency on filtration rate is for filtration rate to decline rapidly above 20 °C, leading, if not soon relieved, to starvation and death (Kim and Powell 2004). Size-dependent assimilation efficiency is also adapted from Hofmann et al. (2006) with a maximum consistent with Powell and Stanton (1985).

For this study, the primary uncertainties in relating maximum size to temperature involve food supply, filtration rate which effectively provides the equivalent uncertainty, and the allocation of assimilated energy to reproduction. A density-dependent stunting of growth consequent of local food limitation might offer an additional explanation for variations in size. Though clearly possible as demonstrated in modeling of high-density populations of bivalves and shown under conditions of husbandry (e.g., Hallam 1965; Powell et al. 1995; Honkoop and Bayne 2002), and although top-down constraints on phytoplankton imposed by bivalve filtering are well-described (e.g., Frechette and Lefaivre 1990; Phelps 1994; Powell et al. 2012), observations of conditions in which bivalve density would be sufficiently high to stunt growth are rarely observed. In the case of *S. solidissima*, densities rarely exceed 1 clam m^{-2} (Stromp et al. 2023). The one possible exception pertinent to *S. solidissima*, in this case for offshore Delmarva as described by Weinberg (1998) who proposed smaller size at the time to be an example of stunting, was likely an unrecognized-at-the-time symptom of warming temperatures. This subsequent conclusion is based on a widespread mortality event in the region shortly thereafter (Kim and Powell 2004; Weinberg et al. 2005) consequent of the 2000 regime shift (Lucey and Nye 2010; Perretti et al. 2017) and a reconsideration of shifting range since the late 1960s by Hofmann et al. (2018).

With respect to the primary uncertainties earlier listed, Hofmann et al. (2006) introduced a two-tiered length-to-weight relationship defining a standard length–weight relationship and a maximal length–weight relationship at peak spawning potential to permit use of condition index to limit the effect of growth at size introduced by an increase in weight due to gametogenesis. Here, the standard length–weight relationship is used, effectively removing the gametogenic effect as it relates to the relationship of assimilation with growth potential. The challenge of food supply and filtration rate is of greater concern. Munroe et al. (2013*a*) clearly showed that estimates of regional primary production, planktonic chlorophyll-content based, do not provide an adequate estimate of food supply for *S. solidissima* (see Holland and Dean 1977; Cognie et al. 2001; Watanabe et al. 2009; Beukema and Dekker 2019 for similar observations); thus, food supply is a critical unknown. Powell et al. (1992) summarized the measured bivalve filtration rates of the time and showed that they fell into two groups, termed by Powell et al. (1992) "high gear" for the faster group and "low gear" for the slower group. Further specification has received considerable attention subsequently, sometimes with controversy (Bayne 2001; Riisgård 2001*a*, 2001*b*; Ehrich and Harris 2015; Keohane et al. 2019), and remains relatively uncertain. This uncertainty, however, is inconsequential in the face of an unknown food supply. As the two competing filtration rates achieve the same output given an appropriate differential in food supply, the high-gear relationship is used in this model.

Thus, in the model employed, differential growth is determined by the temperature dependencies of respiration and ingestion, the latter being the conflation of uncertain filtration rate, but with known temperature dependency, and food supply, with food supply being the primary metric used for model tuning, as filtration rate is assumed invariant across the stock and the temperature dependency is well described. The primary data inputs are bottom water temperature and size–frequency data, from which L can be estimated, as discussed in the following section.

Model calibration

Model calibration requires a known dataset relating maximum size to temperature to determine if the physiology as understood in the afore-referenced model is sufficient to specify temperature–maximum size trends. To do so, the model was specified to identify the size at which the respiratory demand just exceeded the assimilated energy provided under a specified temperature, given a specified food supply. Search increments were 0.1 °C and 1 mm length.

Data resources were obtained as follows. The National Marine Fisheries Service Northeast Fisheries Science Center (NEFSC) conducts a stratified random survey to evaluate the status of the *S. solidissima* stock in the region from Virginia to Georges Bank on a schedule with regional sampling in 2 of every 6 years (Jacobson and Hennen 2019). Further details are in NEFSC (2017). Data on the size frequency of capture for each tow are compiled in 5 mm increments. Data for survey years of 2015–2022 were obtained from NEFSC (2022). The choice of years, besides data availability, was determined by the counterbalance of the rate of warming of the Northwestern Atlantic limiting the viability of data prior to 2015 for application in more recent years and the lifespan of *S. solidissima*, approximately 30 years, as the largest animals will have integrated a time span that covers much of the last two decades of warming temperatures. The NEFSC survey has limited coverage for regions off southern Delmarva. Consequently, additional data, for 2021 and 2023, were obtained from Munroe and Borsetti (unpubl. data; see also Rudders et al. 2024), extending the timeline for analysis to 2023. For each year, tows were assigned to a 10-minute square (TMS = 10 min latitude × 10 min longitude) from 37°N, −76°W eastward and northward to 42.5°N, −67°W, a TMS grid of 54 × 33, with 37°N, −76°W defined as grid [1, 1].

The largest size collected is a poor measure of L, as L represents a relatively central value of animals all of which, theoretically, have reached their maximum size, the variability being a function of genotype (e.g., Hofmann et al. 2006; Hughes et al. 2019) and environmental determinants affecting phenotype (e.g., Evans and Langdon 2006*b*; Hughes et al. 2019). Thus, the largest animal collected in a TMS is a poor estimate of the desired metric. Consequently, the need is to obtain an estimate of the size distribution of the largest clams in as small a geographic space as possible. Given the survey density of the Atlantic surfclam survey and associated information obtained elsewhere, the TMS (10-minute square) is just about as small an area as one can analyze. The analysis is also constrained by the coarseness of the length data available. The NMFS survey data are recorded in 5 cm intervals; consequently, their precision varies across the spectrum of maximum size. A 5 cm difference for a clam of 170 mm is a much smaller proportion than for a clam of 120 mm. Because of the rapidity of warming of the Mid-Atlantic region, and the sensitivity of surfclams to warming temperatures, the dataset is further limited by (a) the need to exclude regions recently colonized and (b) survey data collected prior to 2016. These constraints reduce the number of TMSs that can be evaluated to a small subset of the entirety of the surfclam's range. As the L is not a measure of the size of the largest clam, but rather, a value representative of the range of larger clams in the population, the need is to obtain a subset of all measured clams in a TMS that are representative of the suite of largest clams caught. The fundamental assumption is that this subset represents a range of sizes encompassing the local L for that TMS. The primary uncertainty is to determine how big the subset should be. Expanding the subset offers a tradeoff between the potential of obtaining an improved representation of the size distribution of the largest clams and the potential of including clams that clearly have not reached their maximum growth size.

Consequently, the total number of measurements were enumerated and TMSs with fewer than 25 or 50 measurements in a given year were discarded. The remaining TMSs for the period 2015–2023, totaling 562 containing ≥50 measurements and 687 containing ≥25 measurements for a given year were compiled, and the largest 5 or 10 measurements were averaged across years for each TMS. The average value for each TMS was then declared a reasonable estimate of L for that TMS during the time period from which the data were drawn. The result of this analysis was to assign a known L to each TMS where sufficient data were available over the specified time period. The choice of 25 or 50 total measurements per year per TMS and the choice of averaging the largest 5 or 10 were evaluated using a sensitivity analysis.

Bottom water temperatures were obtained from a ROMS-adapted hydrodynamic model described by Wilkin et al. (2022) and used for *S. solidissima* by Spencer et al. (in press). To agree with previous studies (Munroe et al. 2022; Scheld et al. 2022), bottom temperatures for each TMS were averaged for years 2016–2019. To be pertinent to the time of year providing the most stressful temperatures in the southern part of the range of *S. solidissima*, temperatures obtained for 2016–2019 for each TMS were averaged for the months of August, September, and October. For each TMS where a comparison could be made, an estimated L was obtained from the model based on the average bottom water temperature and compared to the known L derived from data provided by NEFSC (2022), augmented as earlier described. Comparisons were made using several error metrics, including RMSE, the sum of the differences between the observed and expected L, and an average percent error obtained as

$$\frac{\left(\frac{(\text{observed}-\text{expected})}{\text{observed}}\right)}{n}$$

where *observed* is the L estimate from field data, and *expected* is the L estimate from the model; thus, a negative value identifies a model estimate that exceeds the field data. This convention is maintained in all comparisons throughout this study. Note that in evaluating the average percent error, the sensitivity of the comparison is not uniformly distributed across all L estimates, as the original data are in 5 mm size classes: accordingly, a 5 mm error for an L of 170 mm is much smaller than a 5 mm error for a 120 mm L. Thus, sensitivity increases as L decreases. In addition, the number of overestimates and underestimates from this last analysis was also compiled with an expectation that the probabilities would approximate a 50:50 split.

Beginning in the mid-2010s, warming of the Northwestern Atlantic began to produce a range expansion offshore more rapid than the rate of recession of the inshore range of the ocean quahog, *Arctica islandica*, likely due to the ability of ocean quahogs to estivate during the warmer summer and

Fig. 1. Assimilated energy and metabolic respiration requirement (g day^{-1}) at three selected temperatures as a function of length (mm) for a food supply of 0.19 mg L^{-1}. Arrows identify the points where the curves for assimilated energy (dashed line) and metabolic respiration requirement (solid line) cross, establishing maximum size (L).

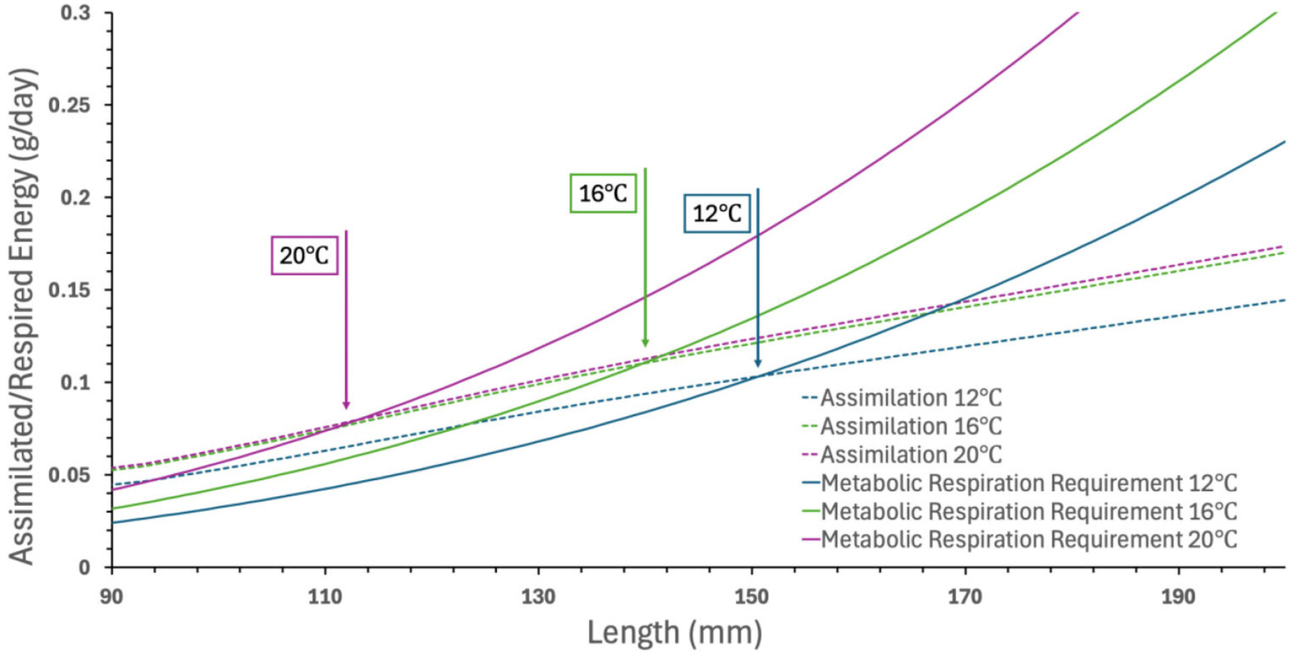

fall months. LeClaire et al. (2024) considered the recessional dynamics of *A. islandica*, including the multi-decadal rate of recession, many times slower than the expansion rate of *S. solidissima*. The resulting rapidly expanding overlap of these two species is well-described (Stromp et al. 2023; Spencer et al. in press). An important consequence is to enable identification of some TMSs where the newly recruited population of *S. solidissima* is unlikely to have reached maximum size as recorded in the NEFSC (2022) dataset, as augmented, whereas the model would estimate maximum size at population equilibrium. Consequently, these TMSs were removed from the dataset.

Besides the potential of offshore bias produced by the rate of *S. solidissima* range expansion, additional geographic biases may be present but not evaluated by the afore-described error metrics. One likely origin would be a nonuniform distribution of available food, a happenstance that might be anticipated given the complex hydrodynamics in the region between Cape Hatteras and Georges Bank (Neuman 1996; Yoder et al. 2002; Mouw and Yoder 2005; Xu et al. 2020; Zang et al. 2021). Accordingly, maps of percent error were examined to identify other sources of geographic bias.

Results

Origin of temperature–size relationship, *Spisula solidissima*

Both ingestion and respiration rates vary with temperature, both nonlinearly, such that growth efficiency slowly declines over time as size increases. Examples of trends of assimilated energy, using specified food supplies of 0.19 and 0.26 mg L^{-1} as examples, and energy expended in respiration as a function of length are shown in Figs. 1 and 2. Where the two curves cross defines L for a given food supply and temperature. Examples of the variability of L thereby identified as a function of temperature given a specified food supply are provided in Fig. 3. The model utilizes such a relationship and the average summer bottom water temperatures to specify an L for each TMS within the temperature range for *S. solidissima*. That range is expanded from Spencer et al. (in press), who included TMSs restricted to an average summer temperature between 11.5 and 18.5 °C, to include TMSs with temperatures as high as 21 °C to show the influence of temperature and food supply on the interaction of L and the 4.75 in (∼120 mm) regulatory size limit presently enforced for Atlantic surfclams (Code of Federal Regulations: CFR 50, §648.75 (b)(3)). This size limit is referred to hereafter as the 120 mm size limit.

Perusal of Fig. 3 shows that the rate at which L declines per degree of increasing temperature for *S. solidissima* is expected to increase as temperatures rise. An explanation for this nonlinearity accrues from the recognition that the driving force behind increments in length is increments in biomass, and the required increment in biomass per increase in length increases with increasing length following a standard allometric relationship with a scaling factor of ∼3, thereby reducing the sensitivity of a change in length as a metric used to identify a physiological response to temperature as length increments. Although over-

Fig. 2. Assimilated energy and metabolic respiration requirement (g day^{-1}) at three selected temperatures as a function of length (mm) for a food supply of 0.26 mg L^{-1}. Arrows identify the points where the curves for assimilated energy (dashed line) and metabolic respiration requirement (solid line) cross, establishing maximum size (*L*).

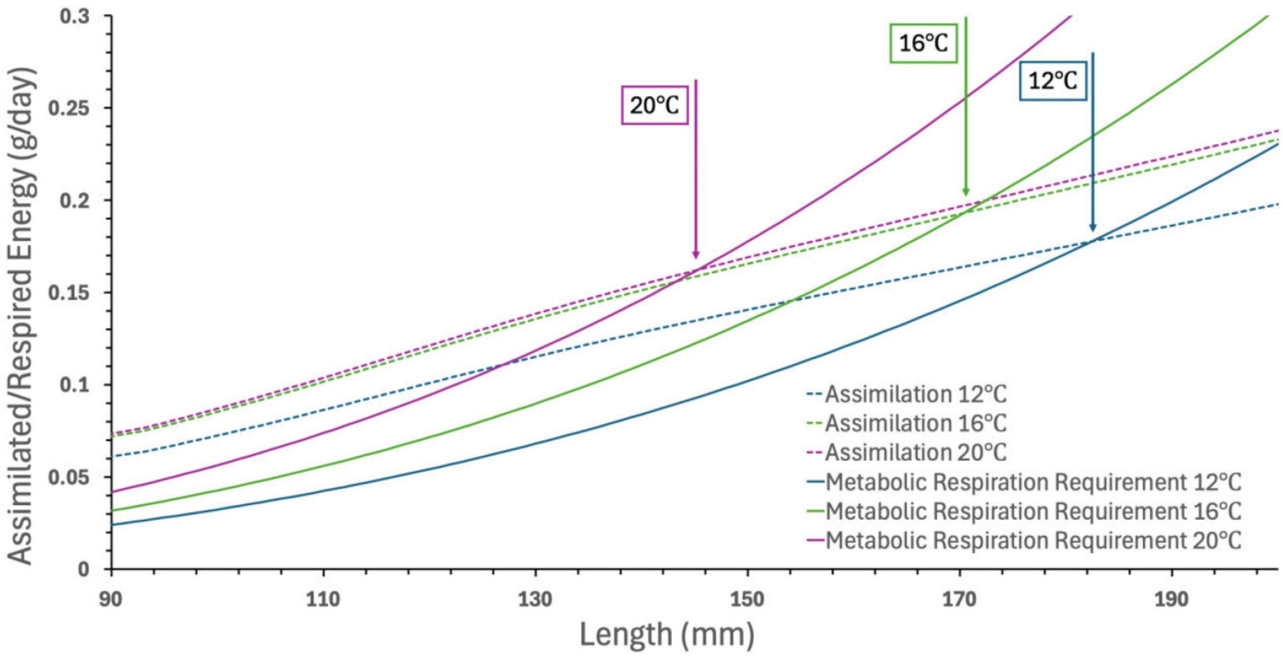

Fig. 3. Length (mm) as a function of temperature given the following food supplies: 0.15 (box), 0.19 (star), 0.26 (circle), and 0.30 mg L^{-1} (diamond). The present-day 120 mm size limit is shown as the black horizontal line.

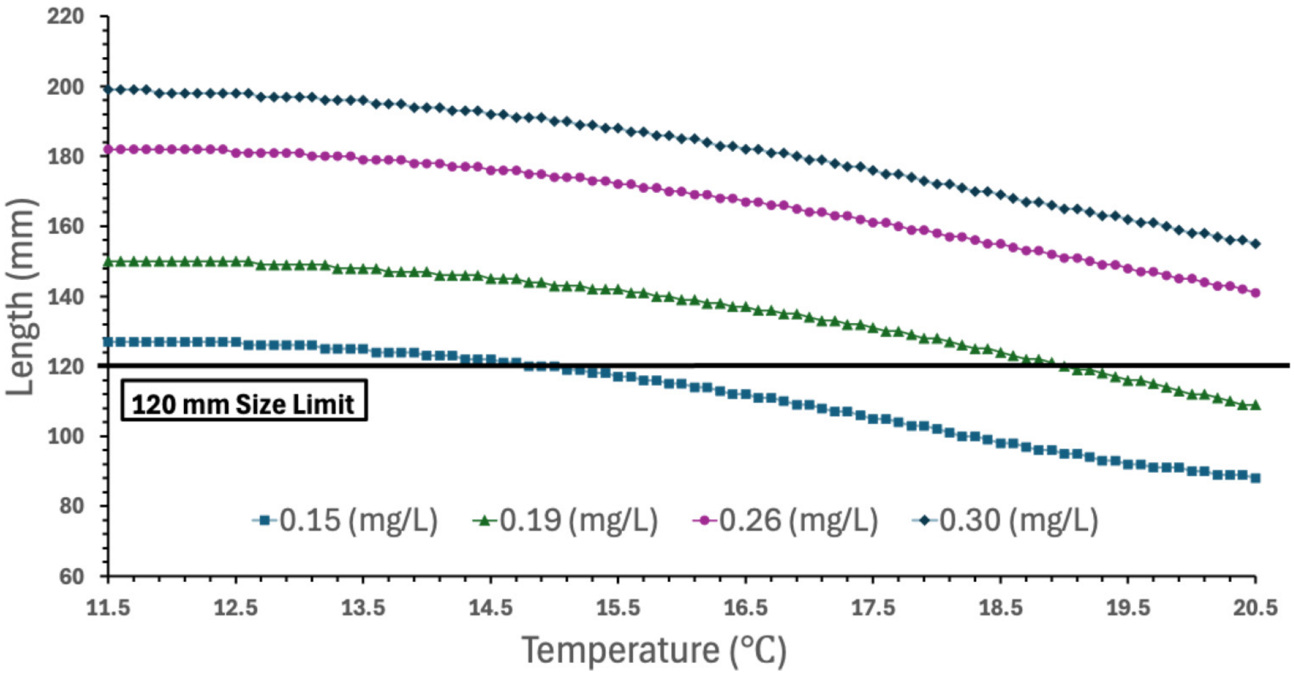

all length–weight relationships for *S. solidissima* are well described (e.g., Marzec et al. 2010), weights for each measured animal in the NEFSC (2022) dataset, as augmented, are not available; accordingly, length rather than biomass has been used.

Development of best-fit model estimate of *L*

Percent error between the observed and model-estimated *L* for each TMS for which data were available from field observations for 2015–2023 is shown in Fig. 4. Error metrics for this and subsequent model estimates are compiled in Table 1.

Fig. 4. Geographic distributions of the average percent error (pDiff) between the observed L and the model-estimated L for the best-case food supply specified as 0.26 mg L^{-1} at the extreme northeast and 0.19 mg L^{-1} at the extreme southwest, with values in between prorated as described in the text. White squares depict the model domain wherein either surfclams are not found or where inadequate data were available for the comparison. Black dots along the shoreline identify primary landing ports for the Atlantic surfclam fishery, from south to north: Ocean City, Maryland; Atlantic City, New Jersey; Pt. Pleasant, New Jersey; New Bedford Massachusetts. Base map obtained from epsg.io; coordinates based on WGS84; map projection based on geocentric translation.

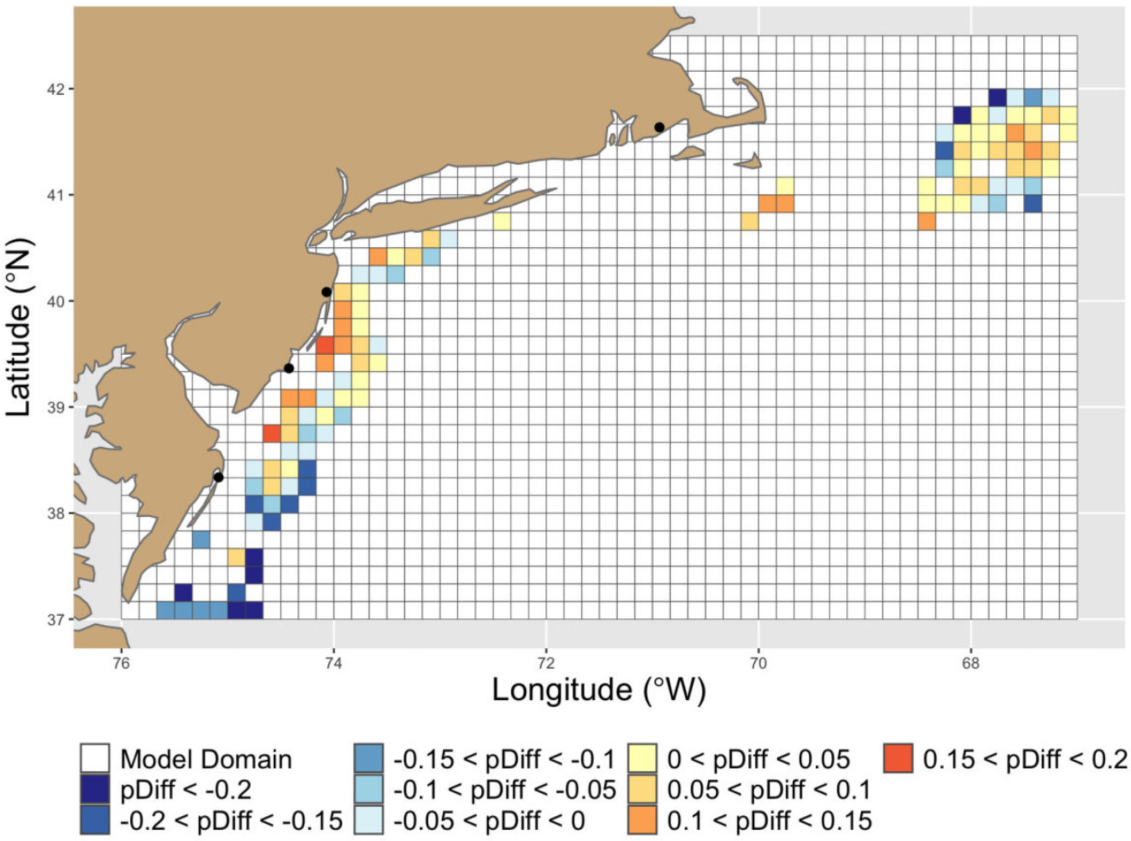

Table 1. Error metrics for selected model estimates for TMSs not including TMSs where ocean quahogs were also found.

Case	N food (mg L^{-1})	S food (mg L^{-1})	Average percent error	Sum of differences	RMSE	Plus	Minus	Figure
25.5	0.19	0.26	0.086	12.561	15.754	62	50	4
25.5	0.19	0.19	0.149	23.495	27.598	92	20	5
25.5	0.26	0.26	0.145	20.029	26.342	39	73	6
25.5	0.15	0.26	0.097	15.345	19.211	87	25	7
25.5	0.19	0.30	0.094	13.573	17.526	27	85	8
25.10	0.19	0.26	0.088	12.319	15.961	54	58	NA
50.5	0.19	0.26	0.086	12.845	15.918	61	38	NA
50.10	0.19	0.26	0.086	12.195	15.656	53	46	NA

Note: Simulations figured are identified by figure number. Definitions of errors are provided in the Methods section. Columns labeled plus and minus tally the number of TMSs in which the L obtained from the NEFSC (2022), as augmented, database exceeded (plus) or fell below (minus) estimates from the model simulation. All food values are in mg L^{-1}. Case identifies the amount of data used for comparisons, as described in the text, with TMSs qualifying if 25 or 50 measurements were made in a tow and using the average of the 5 or 10 largest measurements over all tows in a TMS to obtain an estimate of L.

Primary emphasis was placed on the average percent error and on the proportion of positive and negative comparisons (Table 1). The model estimate depicted in Fig. 4 was obtained in the following steps. An isolated set of 6–10 TMSs for which data were available from field observations for 2015–2023 was identified near the southern inshore edge of the range off Delmarva and near the northern edge of the range on Georges Bank. These were presumed to be characteristic of *S. solidissima* living in regions typified by above average and below average bottom-water temperatures for the stock as a whole. For each of these, a series of food supplies was tested using the defined August–October bottom temperatures for each TMS, and the food supply providing the best L comparison was identified independently for each region.

Fig. 5. Geographic distributions of the average percent error (pDiff) between the observed L and the model-estimated L for a case where food supply was 0.19 mg L^{-1} over the entire domain. White squares depict the model domain wherein either surfclams are not found or where inadequate data were available for the comparison. Black dots along the shoreline identify primary landing ports for the Atlantic surfclam fishery, from south to north: Ocean City, Maryland; Atlantic City, New Jersey; Pt. Pleasant, New Jersey; New Bedford Massachusetts. Base map obtained from epsg.io; coordinates based on WGS84; map projection based on geocentric translation.

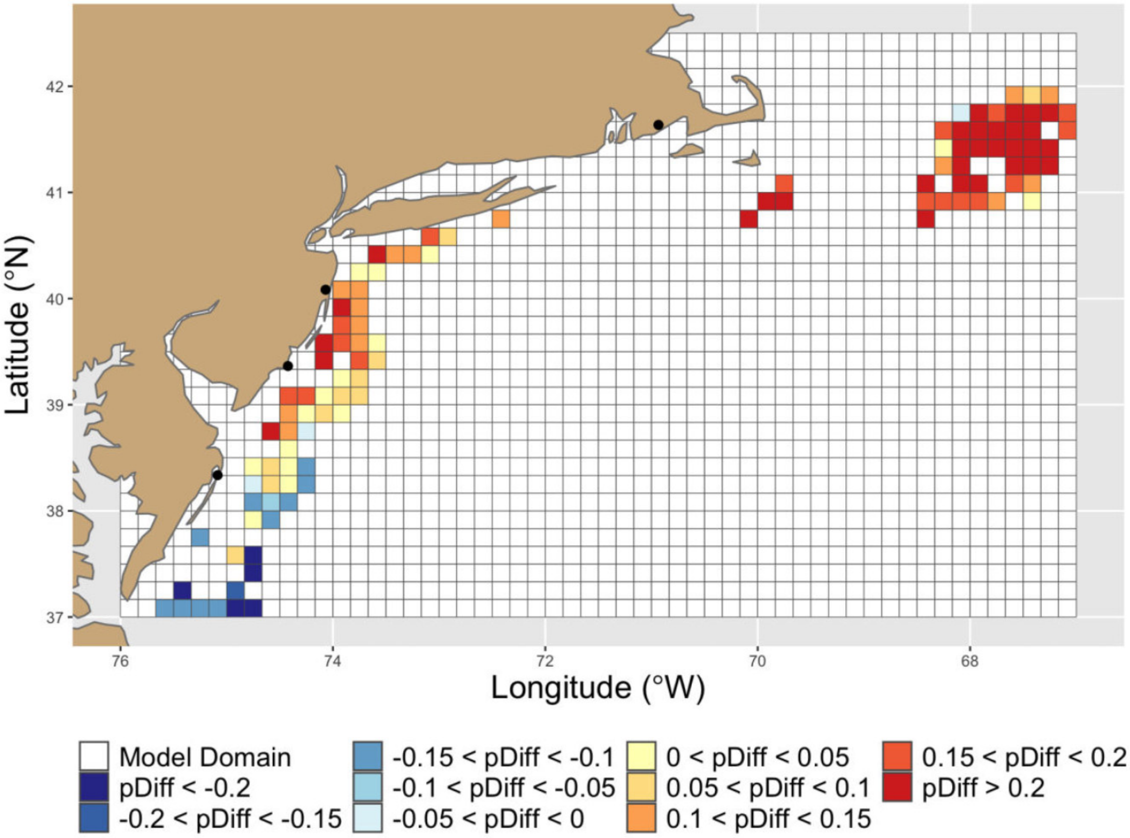

Consistently, the food supply yielding the best fit in the south was lower than the food supply yielding the best fit in the north, an unsurprising outcome as a north–south gradient in planktonic food (inferred from chlorophyll measurements) in this region of the Northwest Atlantic is well described (Neuman 1996; Yoder et al. 2002; Mouw and Yoder 2005). An example model output using the food supply providing the best L estimates for the south, 0.19 mg L^{-1}, shows that the estimate providing the best L estimates for the north is consistently underestimated relative to observations (Fig. 5). The converse, using the food supply for the north of 0.26 mg L^{-1}, shows an overestimate for L in the south (Fig. 6). Accordingly, the L for each TMS for the best case depicted in Fig. 4 was established using a proportional weighting between the northern and southern L values by establishing the angle for each TMS from the horizontal (longitudinal direction), calculating the sine of that angle, and then weighting the northern and southern L values for that TMS by the sine of the angle:

$$h = \sqrt{(y - y_0)^2 + (x - x_0)^2}$$

$$\sin\theta = (y - y_o)/h$$

$$L = (\sin\theta \times L_{N}) + ((1 - \sin\theta) \times L_{S})$$

where $y_0 = 1$, the most southern grid position in the $y = 33$, $x = 54$ grid, and $x_0 = 54$, the most offshore grid position (grid [54, 1]). This weighting scheme provides a continuous angular gradient from the northeast corner (grid [54, 33]) (sin(90) = 1) to the southwest corner (grid [1,1]) (sin(0) = 0) not well specified by latitude or longitude, as the angular geographic boundary of the Mid-Atlantic implicitly integrates the two and provides the additional benefit of avoiding the variation in linear measure implicit in longitude as latitude increases.

The differential in food supply necessitated by Fig. 4 suggests that the food supply in the south is about 73% of that in the north. Unfortunately, as the food supply for Atlantic surfclams is unknown and not directly relatable to surface primary production (Shumway et al. 1994; Reimers et al. 2009; Munroe et al. 2013*a*), as benthic primary production may be the primary food source, the estimated differential cannot be compared to empirical data from the two regions.

Fig. 6. Geographic distributions of the average percent error (pDiff) between the observed L and the model-estimated L for a case where food supply was 0.26 mg L^{-1} over the entire domain. White squares depict the model domain wherein either surfclams are not found or where inadequate data were available for the comparison. Black dots along the shoreline identify primary landing ports for the Atlantic surfclam fishery, from south to north: Ocean City, Maryland; Atlantic City, New Jersey; Pt. Pleasant, New Jersey; New Bedford Massachusetts. Base map obtained from epsg.io; coordinates based on WGS84; map projection based on geocentric translation.

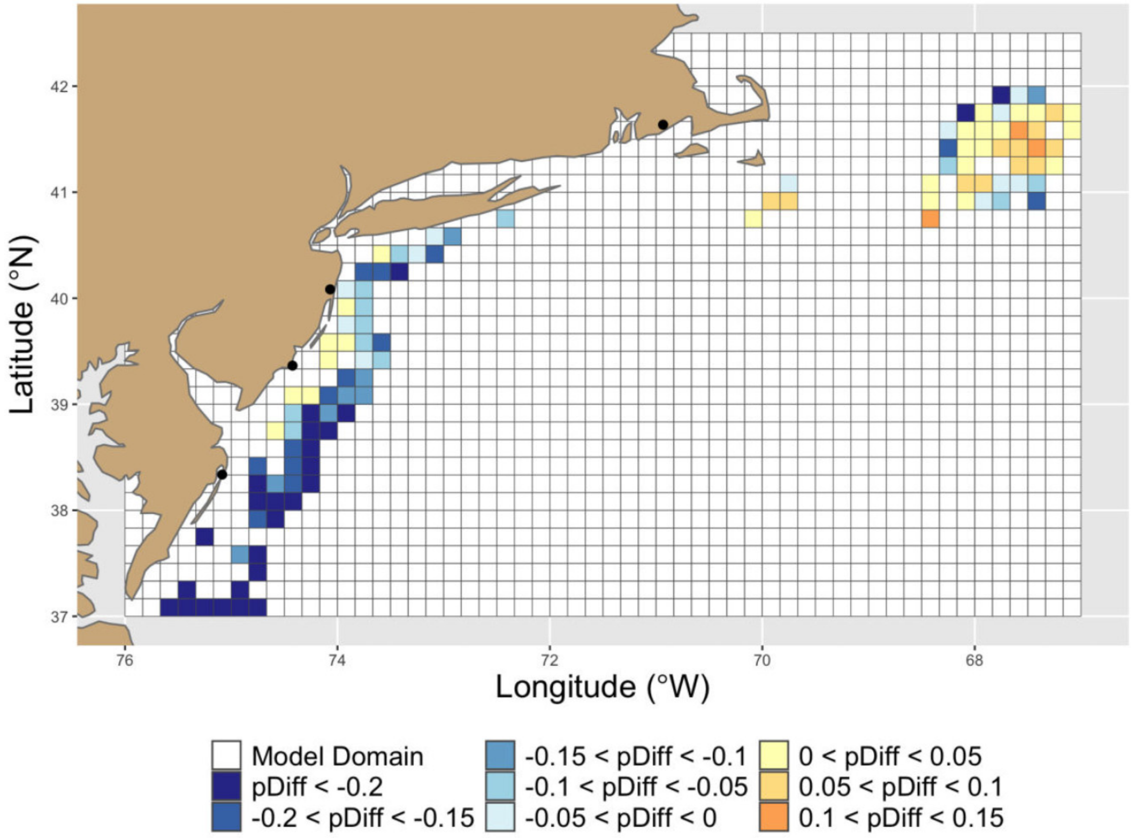

Biases and the influence of sample size on the estimate of L

Final choice of the best model, using food supplies of 0.19 mg L^{-1} in the south and 0.26 mg L^{-1} in the north (Fig. 4), relied on minimizing the error metrics earlier described, particularly the average percent error (Table 1), obtaining a relatively equivalent number of TMSs where the observed L fell above or below the estimated value (Table 1), and mapping of limited regional biases in error distribution (Fig. 4). An evaluation of sample size as a determining factor was accomplished by comparing outcomes of the best-fit estimate obtained after restricting TMSs to those with at least one year with 25 or 50 measured sizes and using the largest 5 or 10 sizes to estimate L. The total number of TMSs evaluated ranged from 99 to 112, depending on the 50- or 25-measurement limit, respectively. Average percent errors varied little, ranging from 8.0% to 9.0% amongst the four comparisons (50/10, 50/5, 25/10, 25/5) (using as an example, food values of 0.19 and 0.26 mg L^{-1} as shown in Table 1). Thus, model estimates were not substantively influenced over a range of sample sizes.

The influence of modest changes in food supply is shown in Figs. 7 and 8. TMSs with error estimates exceeding 15% increase in both cases. Overall, error metrics degrade (Table 1). A modest increase in food supply at the northern end of the range results in increased errors at both ends of the range (Fig. 8). A modest decrease in food supply at the southern end of the range results in increased error in the central portion of the range (Fig. 7). Results are sensitive to variations in food supply, unsurprising given the influence of food supply on bivalve growth routinely being shown to be at least as important as temperature (e.g., Schöne et al. 2005; Montalto et al. 2015; Beukema et al. 2017).

The analysis provided implicitly subsumes the influence of acclimatization to differential temperature regimes on physiological processes (e.g., Rao 1953; Dye 1979; Buxton et al. 1981; Ulrich and Marsh 2008); however, the analysis assumes the absence of genetic selection ameliorating the negative influence of higher temperature on maximum size and fecundity. Bivalves are known to have genotypes offering selective advantage to salinity extremes (Eierman and Hare 2016; McCarty et al. 2020), disease (Yu and Guo 2006; Munroe et

Fig. 7. Geographic distributions of the average percent error (pDiff) between the observed L and the model-estimated L for a case where food supply was specified as 0.26 mg L^{-1} at the extreme northeast and 0.15 mg L^{-1} at the extreme southwest, with values in between prorated as described in the text. White squares depict the model domain wherein either surfclams are not found or where inadequate data were available for the comparison. Black dots along the shoreline identify primary landing ports for the Atlantic surfclam fishery, from south to north: Ocean City, Maryland; Atlantic City, New Jersey; Pt. Pleasant, New Jersey; New Bedford Massachusetts. Base map obtained from epsg.io; coordinates based on WGS84; map projection based on geocentric translation.

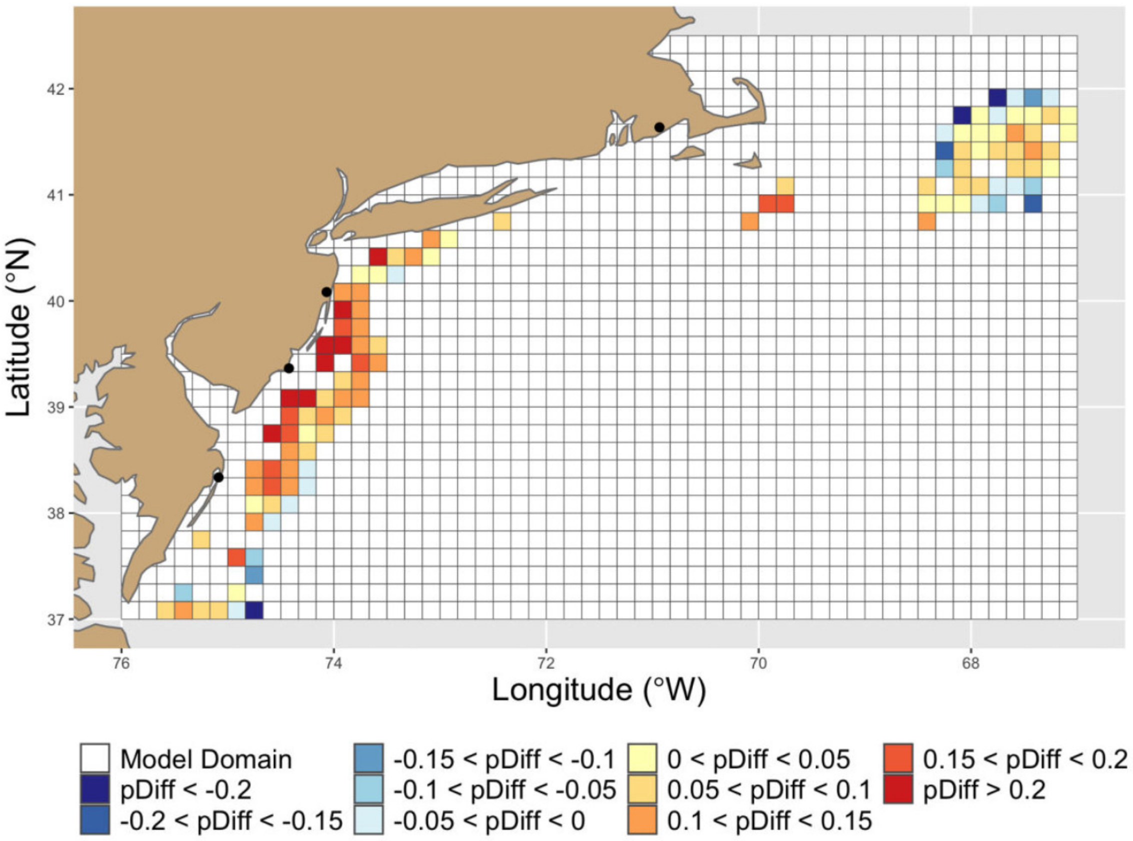

al. 2015), and improved growth (Langdon et al. 2003; Evans and Langdon 2006*a*), and at least inferred for the influence of temperature on spawning (Stauber 1950; Barber et al. 1991; Rio-Portilla and Beaumont 2001). However, apparently little consideration has been given to the potential adaptation of growth rate and maximum size as influenced by temperature. Regardless, genetic adaptation is not included in the present model.

The preferred model (Fig. 4) shows a series of modest biases likely related to the following. (1) Atlantic surfclams are changing their range at a rate much faster than their life span of about 30 years, with the largest animals routinely being 20–25 years old (e.g., Powell et al. 2020*b*), which means that maximum sizes are in part the product of temperatures from years past rather than the time frame used for the model. Overestimates inshore off New Jersey, for example, are consistent with known regions of mortality post-2012 consequent of rising temperatures and associated heatwaves (Pershing et al. 2021; Amaya et al. 2023), suggesting that the surviving animals of large size record earlier cooler periods. Lower condition indices observed by Marzec et al. (2010) also are consistent with this expectation, as the effect of higher temperatures on large animals is to restrict ingestion and thus to lower condition index. (2) Underestimates offshore and in the south are likely due in part to recent recruitment to new habitat (e.g., Stromp et al. 2023; Wisner et al. 2024), the offshore portion of which is likely consequent of the range shift that has happened since 2012. The offshore movement documented by Stromp et al. (2023) is presaged by Weinberg et al. (2005): Wisner et al. (2024) document recent recruitment at the southern end of the range. As a consequence, in some cases, the largest animals measured have yet to achieve maximum size. (3) Higher errors at the southern boundary of the range also are influenced by the small L estimates which exaggerate the difference between the observed and expected values when the original values are known only to within 5 mm. That is, the apparently greater error at the southern extreme of the range is strongly influenced by the allocation of survey observations into 5 mm size classes, enhancing sensitivity of the percent-error metric in this region.

The size–temperature rule: field observations

Figure 9 shows the estimated values of L across the domain occupied by the Atlantic surfclam. Values vary from

Fig. 8. Geographic distributions of the average percent error (pDiff) between the observed L and the model-estimated L for a case where food supply was specified as 0.30 mg L^{-1} at the extreme northeast and 0.19 mg L^{-1} at the extreme southwest, with values in between prorated as described in the text. White squares depict the model domain wherein either surfclams are not found or where inadequate data were available for the comparison. Black dots along the shoreline identify primary landing ports for the Atlantic surfclam fishery, from south to north: Ocean City, Maryland; Atlantic City, New Jersey; Pt. Pleasant, New Jersey; New Bedford Massachusetts. Base map obtained from epsg.io; coordinates based on WGS84; map projection based on geocentric translation.

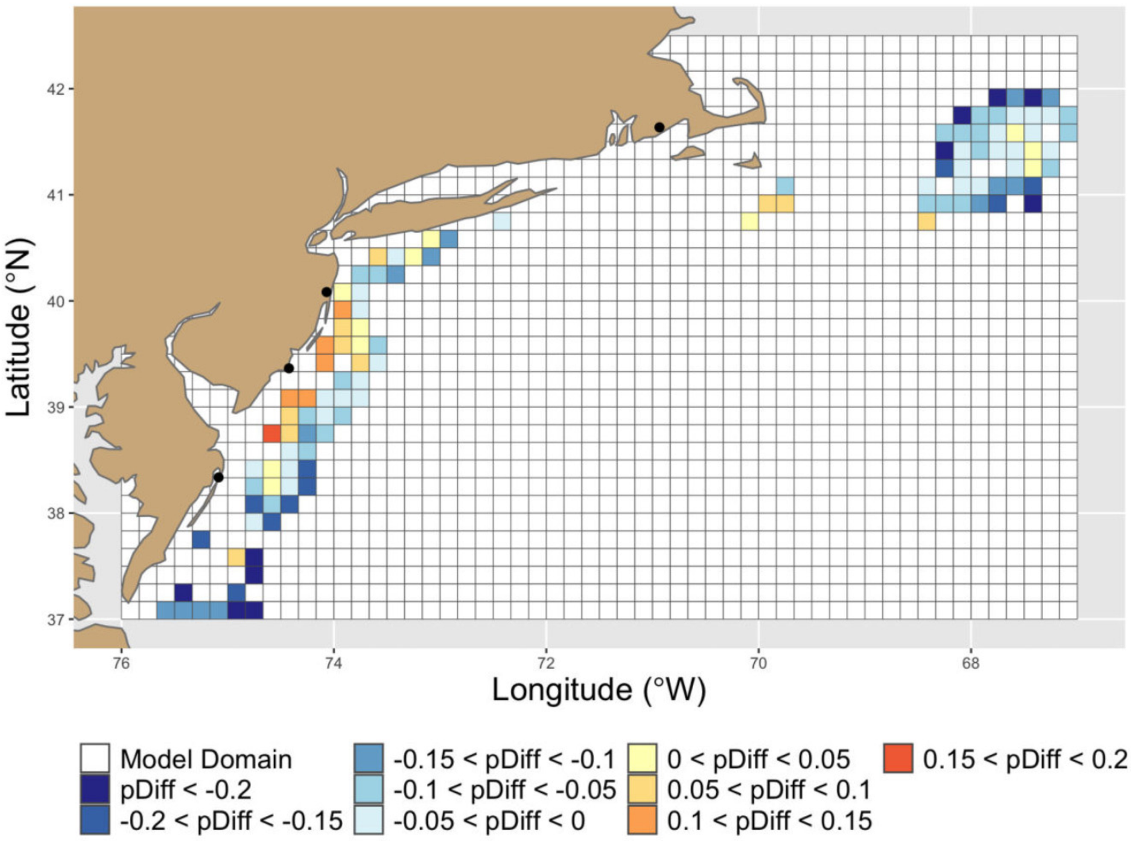

about 100 mm in the extreme inshore at the southern extent of the range, rising to about 150 mm offshore. Values off New Jersey vary from about 125 mm inshore to 160 mm offshore. Sizes exceeding 170 mm are not seen west of central Long Island and only reach or exceed 180 mm near the Great South Channel and on the deeper regions of Georges Bank.

The model identifies two critical determinants of Atlantic surfclam maximum size in any TMS, setting aside the truncated demographics imposed by recent recruitment into new habitat: temperature and food supply. These results are unsurprising given the necessity of their inclusion into any forward-projecting population dynamics model and the common observation of clinal size variation with latitude in bivalves (Nicol 1964; Lomovasky et al. 2011), including Atlantic surfclams (Chute et al. 2016; Munroe et al. 2016). The limited number of observed cases in the literature documenting a temperature–size rule in Bivalvia empirically suggests that factors such as food supply often limit detection of temperature effects on maximum size.

Figure 10 provides empirical support for the effect of temperature on *S. solidissima* using the NEFSC (2022), as augmented, database supporting model simulations reported herein and bottom water temperatures obtained as described by Spencer et al. (in press). To obtain this figure, data for the eastern half of the domain, Block Island to Georges Bank, were excluded. This removes from the dataset data for the region of southern New England and Georges Bank, where larger sizes are encountered in routinely cooler waters, well documented by Munroe et al. (2016), Diaz et al. (2024), and Powell et al. (2020*b*), and predicted herein (Fig. 9), where little size variation occurs, where length becomes a less sensitive metric to track responses to temperature due to the larger sizes, and likely, as shown herein, where large size is partially due to enhanced food supply. The remaining data provided in Fig. 10 include all TMSs outside of the known ecotone with ocean quahogs, wherein recent recruitment likely influences maximum size (Stromp et al. 2023). Figure 10 records 84 size-temperature pairs and demonstrates a modest correlation with size declining with increasing summer temperatures ($R^2 = 0.183$).

To further evaluate the data supporting Fig. 10, the dispersion of points was split into octamerous units by the quar-

Fig. 9. Projections of L for the period 2016–2019 based on the model specified in Fig. 4. White squares depict the model domain wherein either surfclams are not found or where inadequate data were available for the comparison. Black dots along the shoreline identify primary landing ports for the Atlantic surfclam fishery, from south to north: Ocean City, Maryland; Atlantic City, New Jersey; Pt. Pleasant, New Jersey; New Bedford Massachusetts. Base map obtained from epsg.io; coordinates based on WGS84; map projection based on geocentric translation.

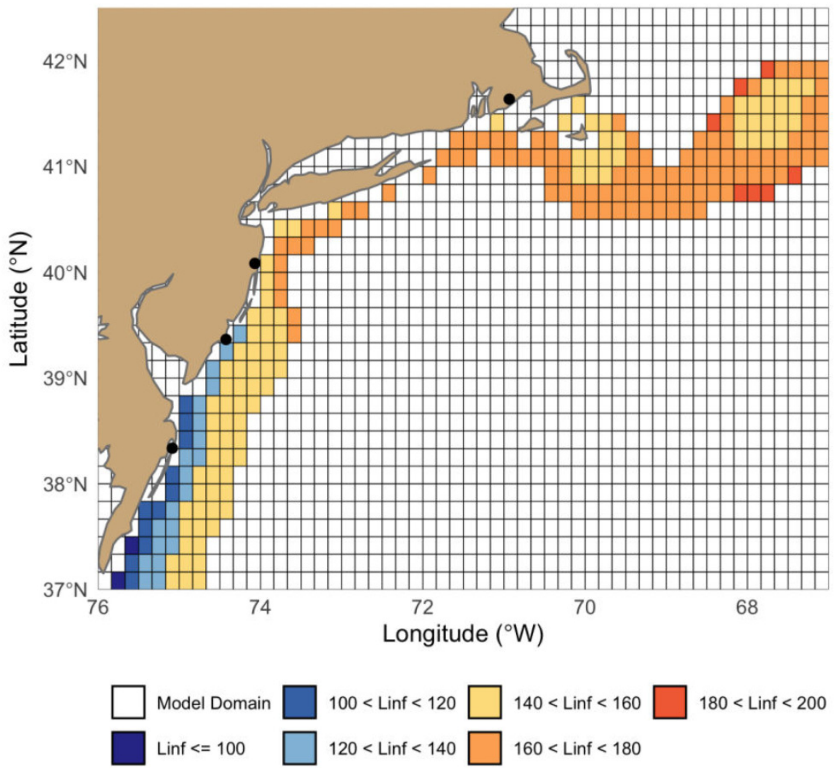

tiles of maximum size and August–October bottom temperature, yielding 16 octiles each with an expected occupation by data points of 0.0625. The number of points falling into each octile was evaluated relative to the expectation of a random dispersion of points amongst the 16 octiles using a binomial test. Occupation in three octiles differed from expectation. Setting octile [x, y] to [1, 1] at the lower left in Fig. 10, octiles [1, 1] and [4, 2] had fewer TMSs than expected by chance ($P < 0.05$). Octile [4, 1] had significantly more TMSs than expected by chance ($0.001 < P < 0.005$). Thus, smaller maximum sizes are more likely to occur at higher temperatures and less likely to occur at lower temperatures in the region of western Long Island to southern Delmarva, in agreement with the expectation from the temperature–size rule, and model estimates (Fig. 10). The absence of a significant dispersion at temperatures of ≤15 °C, commonly yielding maximum sizes of 150+ mm, is in part explained by Fig. 3 which shows that the variation in linear size with temperature is strongest at temperatures above 15 °C. This is a consequence of the increasing poverty of length as a useful metric for metabolic processes as size increases, an outcome required by the allometric relationship between length and biomass. That is, at sizes of 150+ mm, larger increments in biomass are required to produce small increments in linear size (Marzec et al. 2010), resulting in a decreased temperature signal using a length-based metric at lower temperatures. The temperature signal, at lower temperatures, is consequently more readily obfuscated by other factors affecting maximum size, particularly food supply.

An additional examination of size–temperature trends can be accessed by identifying TMSs with sufficient measurements in the NEFSC (2022), as augmented, database for 1997–1999 compared to 2016–2023. The trend in increased temperature over this score of years in this region is well documented (Lucey and Nye 2010; Friedland et al. 2020, 2022). A comparison between estimates of L using the NEFSC (2022), as augmented, database for these two time segments shows that maximum size in these collections has declined in 16 of 24, an incidence higher than expected by chance (binomial test; $P = 0.04$) (Fig. 11). Amongst the southernmost half, essentially the region of the Mid-Atlantic Bight off New Jersey and Delmarva, 11 of 12 TMSs are characterized by a decline in Atlantic surfclam size, an unlikely event given an expectation of a 50:50 split (binomial test: $P = 0.003$) (Fig. 11). Of these, the least size differential is 15 mm, itself a substantial shift in maximum size. In the northernmost half, approximating extreme northern New Jersey, Long Island, and southern New England shelf, more than half of the TMSs are characterized by increased size, and an even higher percentage (4 of 5) are so characterized on Georges Bank

Fig. 10. Ordinary least squares regression of length (L estimates in mm) versus bottom water temperature for TMSs west of Georges Bank, including western Long Island, New Jersey, and Delmarva, but not including TMSs in which ocean quahogs were found. Lengths are extracted from the NEFSC (2022), as augmented, database as described in the Methods section. Bottom temperatures are obtained as described by Spencer et al. (in press). The orange lines represent the 25% percentile, green lines represent the median, and purple lines represent the 75% percentile of the data distribution relative to length and temperature. The regression line is L (mm) $= -4.93$ T($^{\circ}$C) $+ 222.62$ ($R^2 = 0.183$).

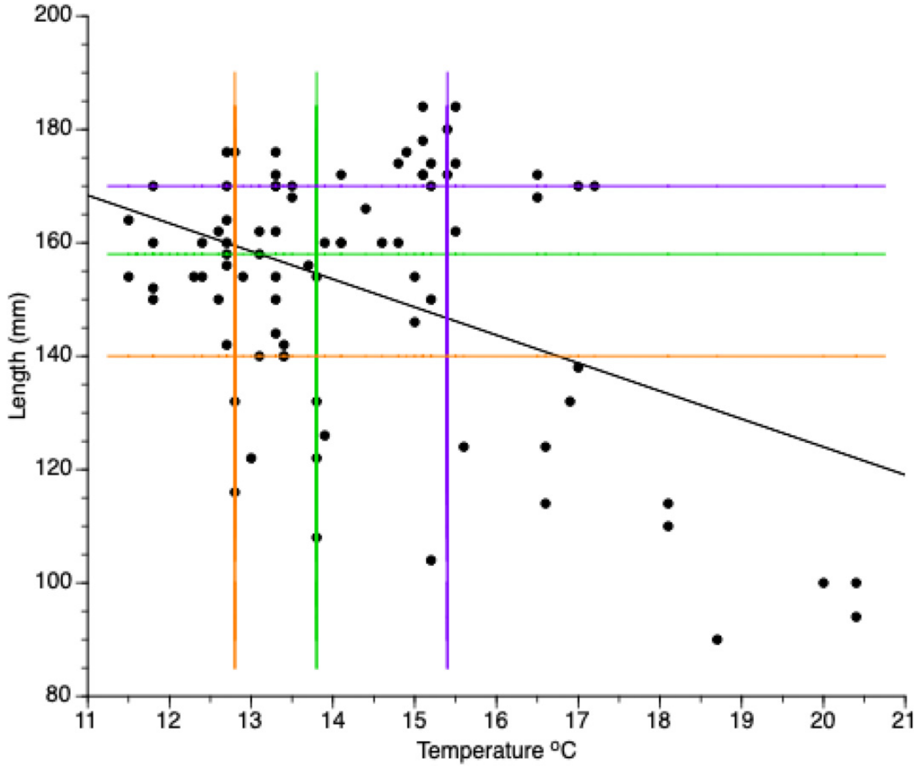

(Fig. 12). As the Mid-Atlantic Bight has warmed, Atlantic surfclam sizes have fallen in the south consistent with the expectations from Figs. 1, 2, and 10 and consistent with model estimates shown in Fig. 9. The tendency for increased size in the north is more difficult to explain as cooler waters should have already supported a larger size. One option is that these TMSs mark locations earlier too cold for Atlantic surfclams, but where range expansion in the near past as provided cohorts that have increased in size over the intervening decades. Timbs et al. (2019) document a shift of Atlantic surfclams into deeper water in this region, and Powell et al. (2020*b*) provide a pertinent example for the region east of Nantucket.

Discussion

The temperature–size rule, von Bertalanffy growth, and fecundity

Of concern is the degree to which the temperature–size rule, as modified by variations in food supply, is a primary determinant of the size–frequency distribution relative to competing factors such as size- or age-dependent natural mortality rates and size truncation by fishing. Since at least the time of Pütter (1920) and von Bertalanffy (1938), the influence of the differential allometric scalings of surface-area-dependent and volume-dependent processes has received scrutiny as an explanation for a range of phenomena dependent upon measures of size. The widespread presence of a relationship between maximum size and temperature is well-described for a vast host of gill-bearing species with a range of potential explanations, commonly including the limitation of gill surface area in the uptake of oxygen (Mills et al. 2024; Sampognaro and Segura 2024; Lavin et al. 2022; Pauly et al. 2022). Although the same limitation might be anticipated in bivalves, the dominance of the gill as a feeding organ in comparison to a ventilatory organ (Jørgensen et al. 1986) places a more profound physiological limit on metabolic energetics. As a consequence, temperature and food supply exert a primary control and together determine maximum size, expressed normally for bivalves by the von Bertalanffy parameter L .

Jensen (1997) identified an inverse relationship between the growth rate as expressed by the von Bertalanffy parameter K (Brody's K[1]) and L . This inverse relationship is anticipated by the influence of temperature accelerating growth at small size and disproportionately capping growth

---

[1] The origin of the moniker precedes Brody (1945). Weymouth et al. (1931) use the identifier and recognized Brody et al. (1923) as the basis for the eponymy.

Fig. 11. The differential in length (mm) between the *L* obtained for the years 1997–1999 from the NEFSC (2022), as augmented, database and the *L* obtained for the years 2016–2023 from the same database for the region west of Georges Bank, including Long Island, New Jersey, and Delmarva. Comparisons are based exclusively on observation data. Positive numbers indicate a larger length for the 1997–1999 period. Thus, a value of 15 indicates that the *L* for years 1997–1999 was 15 mm larger than the *L* for years 2016–2023. Partitions identify the medians. Grid cell numbers on the axes as defined in the text are in 10 min intervals with cell [1, 1} located at latitude 37°N and longitude −76°W. Note that latitude increments with increasing grid number on the *y*-axis from 37°N to 39.5°N, and longitude increments with increasing grid number on the *x*-axis from −76°W to −74°W.

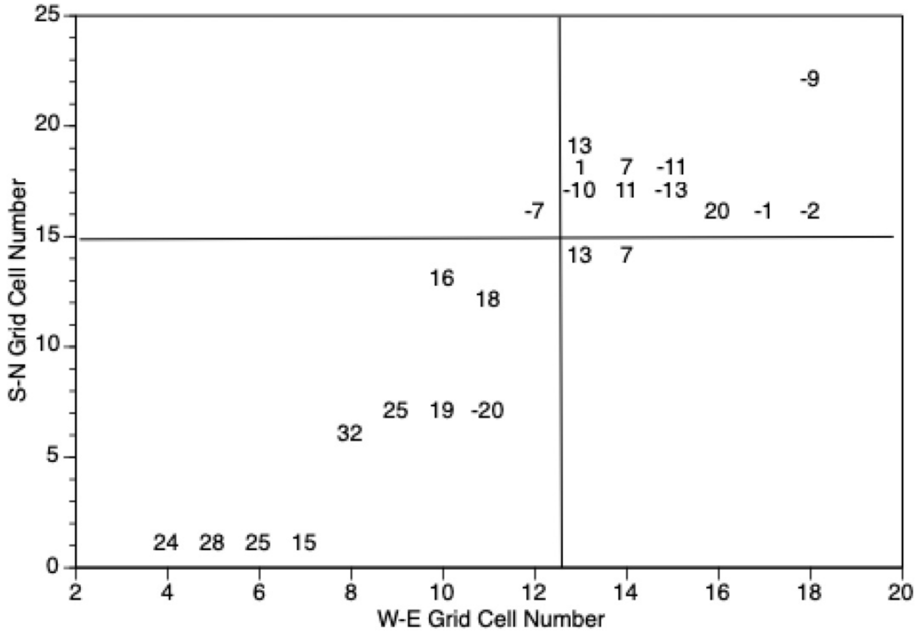

at large size and is both anticipated theoretically (e.g., Klinck et al. 2023) and observed (Weymouth et al. 1931; Bauer 1992; Borsetti et al. 2021; Queiros et al. 2024). Information gathered from datasets summarized by Munroe et al. (2016) and NEFSC (2022) yielded an analogous relationship (Spencer et al. in press) reproduced here

$$K = 0\ 8144 - 0\ 0035 \times L$$

Although considerable variability exists (see also Weinberg 1998; Chintala and Grassle 2001; Diaz et al. 2024), the relationship is clearly inverse. Taking the derivative of the von Bertalanffy equation specifies the growth rate as

$$G\,(\mathrm{A}) = \mathrm{KL}\quad \mathrm{e}^{-\mathrm{KA}}$$

where *G* is the growth rate and *A* is age. The growth rate at birth (settlement) is

$$\mathrm{G}\,(\mathrm{A} = 0) = \mathrm{KL}$$

which is the largest growth rate (see also Calow 1977). Assuming the von Bertalanffy growth model adequately describes bivalve growth, any process supporting an increase in *L* should be accompanied by a decrease in ontogenetic growth rate, which is observed. The inverse relationship in the case of the Atlantic surfclam is determined by the differential temperature dependencies of assimilation and respiration (Fig. 3). In essence, at higher temperatures, juvenile growth efficiency is higher relative to respiration than at cooler temperatures, but respiration rate rises more rapidly due to the higher temperatures, thereby more quickly capping maximum size.

The inverse relationship of growth rate and *L* has considerable impact on lifetime fecundity, an important parameter related to fitness (Bell 1980; Baskett et al. 2005; Charnov et al. 2007). Based on the relationships expressed in Figs. 1, 2, and 3 relating size to temperature, a relationship between lifetime fecundity and temperature can be expressed, given a few assumptions. Besides the recurring caution related to food supply and filtration rate, for any temperature–size relationship defined under a specified assimilation rate, the principal uncertainty is the allocation of energy to gametogenesis. Typically, that allocation can be expressed in terms of the gamete fraction of body weight upon spawning; however, this fraction is notoriously variable within the bivalves (Powell and Stanton 1985), with *Crassostrea gigas* probably holding the record with a gamete fraction near 50% (Kang et al. 2003; Cardoso et al. 2013). More commonly, the gamete fraction falls near 20%–25% (Powell and Stanton 1985). The gamete fraction for *S. solidissima* is unknown; for convenience, a value of 20% is used here. Several bivalve modeling efforts have incorporated explicitly or implicitly the possibility that the largest animals may have a reduced rate of egg production per gram either due to a direct constraint on gamete fraction at large size or to a restriction in the frequency of spawning (e.g., Choi et al. 1994; Hofmann et al. 2006). Although assumed by Munroe et al. (2013*a*), the relationship has not

Fig. 12. The differential in length (mm) between the L obtained for the years 1997–1999 from the NEFSC (2022), as augmented, database and the L obtained for the years 2016–2023 from the same database for Georges Bank. Comparisons are based exclusively on observation data. Positive numbers indicate a larger length for the 1997–1999 period. Thus, a value of −19 indicates that the L for years 1997–1999 was 19 mm smaller than the L for years 2016–2023. Partitions identify the medians. Grid cell numbers on the axes as defined in the text are in 10 min intervals with cell [1, 1} located at latitude 37°N and longitude −76°W. Note that latitude increments with increasing grid number on the *y*-axis from 39.7°N to 40.1°N, and longitude increments with increasing grid number on the *x*-axis from −71.2°W to −50.2°W.

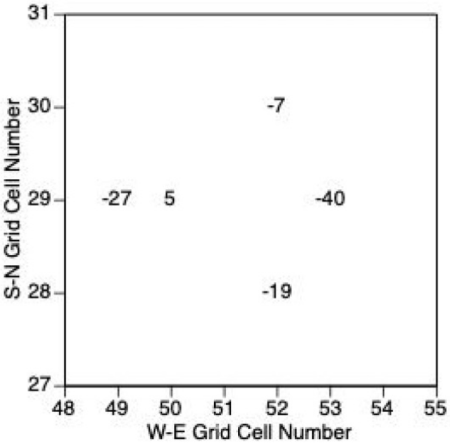

been shown for *S. solidissima* and a declining gamete fraction at larger size is not included in estimates provided here. For convenience, calculations assume a cohort of 100 individuals, a natural mortality rate of 0.15 year^{-1} as specified by NEFSC (2022), assuming 1% of the cohort remains at the lifespan of 30 years (Hoenig 1983), and a fishing mortality rate of 0.015 year^{-1} (see NEFSC 2017) assuming a fully selected size of 100 mm. Spawning for Atlantic surfclams often includes a late spring/early summer spawn and a fall spawn (Ropes 1968; Jones 1981). The degree to which temperature influences the timing and number of spawns per year is poorly known. Calculations assume one spawn per year. Relationships specifically used include:

$$L_a = L\ \left(1 - e^{-ka}\right)$$
$$W_a = \alpha L_a^{\beta}$$
$$N_a = N_0 e^{-(m+f)a}$$
$$G_a = N_a W_a \mathrm{E}$$
$$\text{Lifetime Fecundity} = \sum_{a=\text{mat or sl}}^{a=a_{\max}} G_a$$

where L is length (mm), L is the maximum size based on a stipulated temperature (mm), a is age (years), k is Brody's K (year^{-1}), W is flesh weight (gm), α and β are allometric parameters, N_0 is the number of females born into the cohort, m is the natural mortality rate (year^{-1}), f is the fishing mortality rate (year^{-1}), E is the gamete fraction, mat is the age at maturity (years), sl is the age at the size limit (years), $a_{\max}$ is the maximum age (years), and G is the egg production (gm).

Figure 13 shows that lifetime fecundity declines with increasing temperature. Lifetime fecundity is determined primarily by the number of years at large size which is influenced by the size at L and the rapidity of growth to that size as specified by Brody's K. As temperature increases, the more rapid early growth rate (higher Brody's K) does not counterweigh the cap on size imposed by the temperature effect on L. Variations in food supply scale the effect. The pattern is retained regardless of the inclusion of fishing; in this case a representative fishing mortality rate of 0.015 year^{-1} is used in comparison to the no-fishing case (NEFSC 2022). Thus, higher temperatures rob the species of reproductive potential, assuming, of course, the appropriateness of the conditions for calculation as specified.

Management implications and the temperature–size rule: catch size-limits in bivalves

Size limits have been used for fisheries management to restrain total catch and to limit recruitment overfishing (e.g., Williams and Blood 2003; Henderson 2009; Powell et al. 2010), in turn often accompanied by increased discard mortality (e.g., Borges et al. 2006; Coggins et al. 2007; Powell et al. 2011). Although some have examined size limits as they influence population dynamics (van Wynsberge et al. 2013; McIntyre et al. 2015; Moore et al. 2016; LeDoux et al. 2023), size limits in shellfisheries are often imposed to maintain size consistency in the marketplace (Berrigan et al. 1991; Powell et al. 2005; Bald et al. 2009), and market forces may impose size limits de facto (Powell et al. 2005). Overall, rigorous evaluation of the use of size limits in managing shellfisheries has been rare (e.g., Kraeuter et al. 2008; Moore et al. 2016). The challenge in using size limits to restrict harvest for the purposes of supporting sustainable management is the commonplace maturity at sizes well below maximum size and well below marketable size (e.g., Powell and Stanton 1985), permitting spawning to begin months to years prior to recruitment into the fishery, and the absence of a relationship between broodstock and recruitment (Hancock 1973), except in a few unusual circumstances (e.g., for oysters—Hemeon et al. 2020; for abalone—Harford et al. 2019; for scallops—Munroe et al. 2018; for whelk—Borsetti et al. 2018: but see examples of severe overfishing imposing a broodstock limitation; Peterson and Summerson 1992; Peterson 2002; Kraeuter et al. 2005).

A consideration of the influence of the temperature–size rule with respect to the usability of a size limit to benefit population dynamics and sustainable management has not occurred. *Spisula solidissima* is a prototypical bivalve in several respects relative to the conundrum of the potential use of size limits in management exclusive of regulating size in the marketplace. Bivalves mature at size, not age (Powell and Stanton 1985). *Spisula solidissima* matures in its first year (Chintala and Grassle 1995) at a size much smaller than anticipated from bivalves as a whole (Powell and Stanton 1985) and well below the size typically fully selected by the gear (100–120 mm; NEFSC 2017). A broodstock–recruitment rela-

Fig. 13. Lifetime fecundity for cohorts living at designated temperatures under the proviso that the natural mortality rate is 0.15 year^{-1}, under stipulated food supplies of 0.15 mg L^{-1} (purple), 0.19 mg L^{-1} (dark blue), 0.26 mg L^{-1} (dark green), and 0.30 mg L^{-1} (light blue), with and without fishing. Fishing mortality rate is set at 0.015 year^{-1} for the comparisons to $F = 0$. Maturity is set at 35 mm. In each case, von Bertalanffy parameter L increases and k decreases as temperature declines as modulated by food supply (see earlier figures). Steps in each line originate from the interaction of an assumed 1-spawn per year time step with the growth rate.

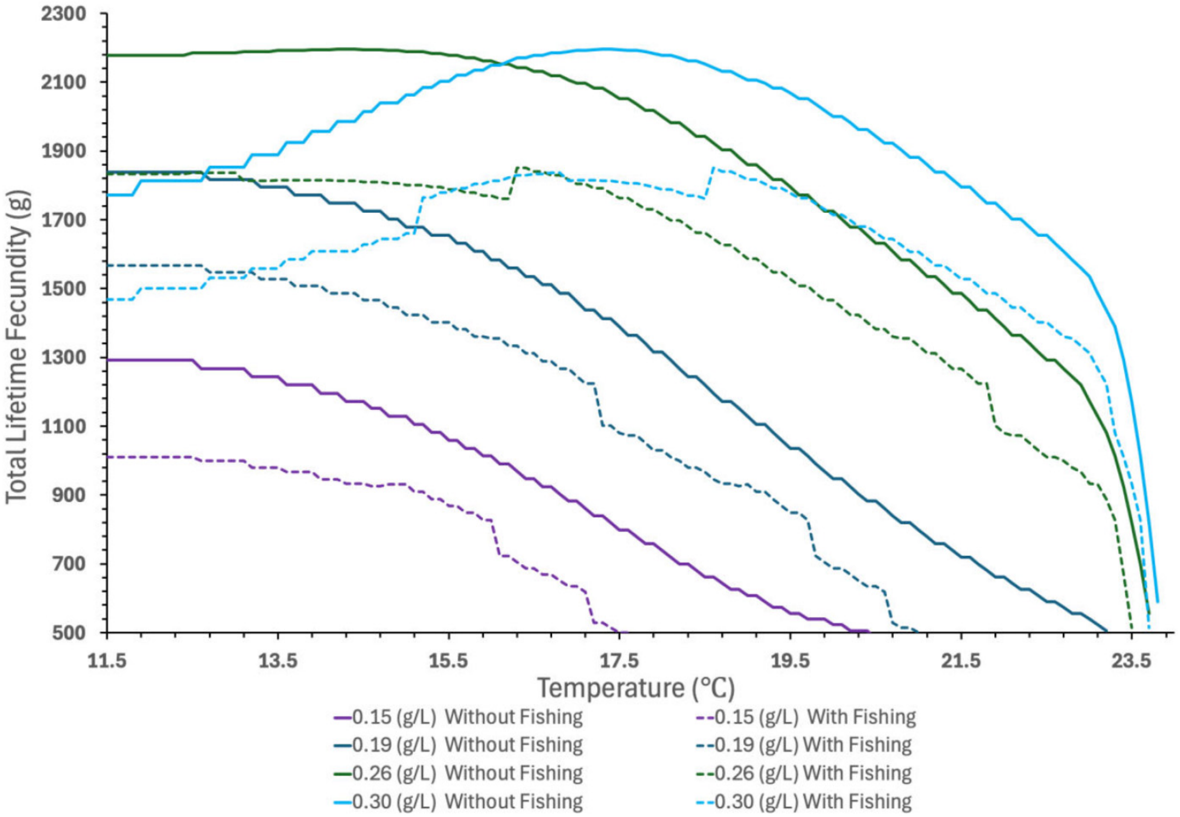

tionship does not exist (Timbs et al. 2018; NEFSC 2022); steepness is estimated at 0.95 (NEFSC 2022; Hennen et al. 2018). Recruitment is shown to be influenced by larval supply (Ma et al. 2006; Czaja et al. 2023) but early post-settlement survival is a primary determinant (Quijón et al. 2007; Timbs et al. 2018), as is often the case for bivalves (Powell et al. 1994; Ólafsson et al. 1994; Beukema and Dekker 2019). Consequently, population fecundity is unlikely to directly influence recruitment, and particularly recruitment into the fishery.

For Atlantic surfclams, a regulatory size limit is set at 4.75 in (120.65 mm). Figure 14 shows a comparison of lifetime fecundity focused on the fraction of lifetime fecundity retained by avoiding capture in the size range of 100–120 mm, assuming a fishing mortality rate of 0.015 year^{-1}, consistent with observations (NEFSC 2022), and imposing a 100 mm knife-edge dredge selectivity. For most hydraulic dredges, selectivity drops precipitously at sizes less than 100 mm. The estimation of the impact of the 120 mm size limit on lifetime fecundity assumes that smaller animals are not boarded or that discards have high survival. Discard mortality is unmeasured for Atlantic surfclams and is likely highly variable depending on the design of sorting machinery on the fishing vessel (e.g., roller table vs. shaker table). Here, 100% survival of discards is assumed.

The influence of a size limit increases rapidly once the maximum size permitted physiologically drops close to the size limit. The total contribution to fecundity by a cohort of 100 individuals, however, also declines substantively (Fig. 13). Over much of the temperature range, the Atlantic surfclam fishery reduces lifetime fecundity by about 10%–20%. This stability accrues from the primary loss being contributed by the larger animals targeted by the fishery: some of these animals otherwise would live for many additional years and provide substantive egg production during that portion of their lifetime. In comparison, the largest proportional benefit of a size limit accrues in regions where the temperature–size rule restricts lifetime fecundity. In the case of the Atlantic surfclam, that region of greatest influence is the region where temperatures rise to 18–20 °C, temperatures very near the high-temperature limit of the species' range (Spencer et al. in press), leaving little leeway for the size limit to influence the sustainability of the stock. In other words, lifetime fecundity is limited when maximum size is limited and, although a size limit increases potential egg production, that increase is also limited. In addition, as food supply increases, the importance

Fig. 14. The fraction of lifetime fecundity retained in the fished population by a 120 mm size limit, based on a natural mortality rate of 0.15 year^{-1}, a fishing mortality rate of 0.015 year^{-1}, and a knife edge selectivity for the fishery at 100 mm, assuming food supplies of 0.18, 0.19, and 0.20 mg L^{-1}. If the 120 mm size limit was completely ineffective, a value of 0 would be obtained. See Fig. 13 for further specifications. Note that the jaggedness of the plot originates from the assumption of one spawn per year, which imposes steps of varying dimensions depending on the precise timing of the increments in age within and between size classes.

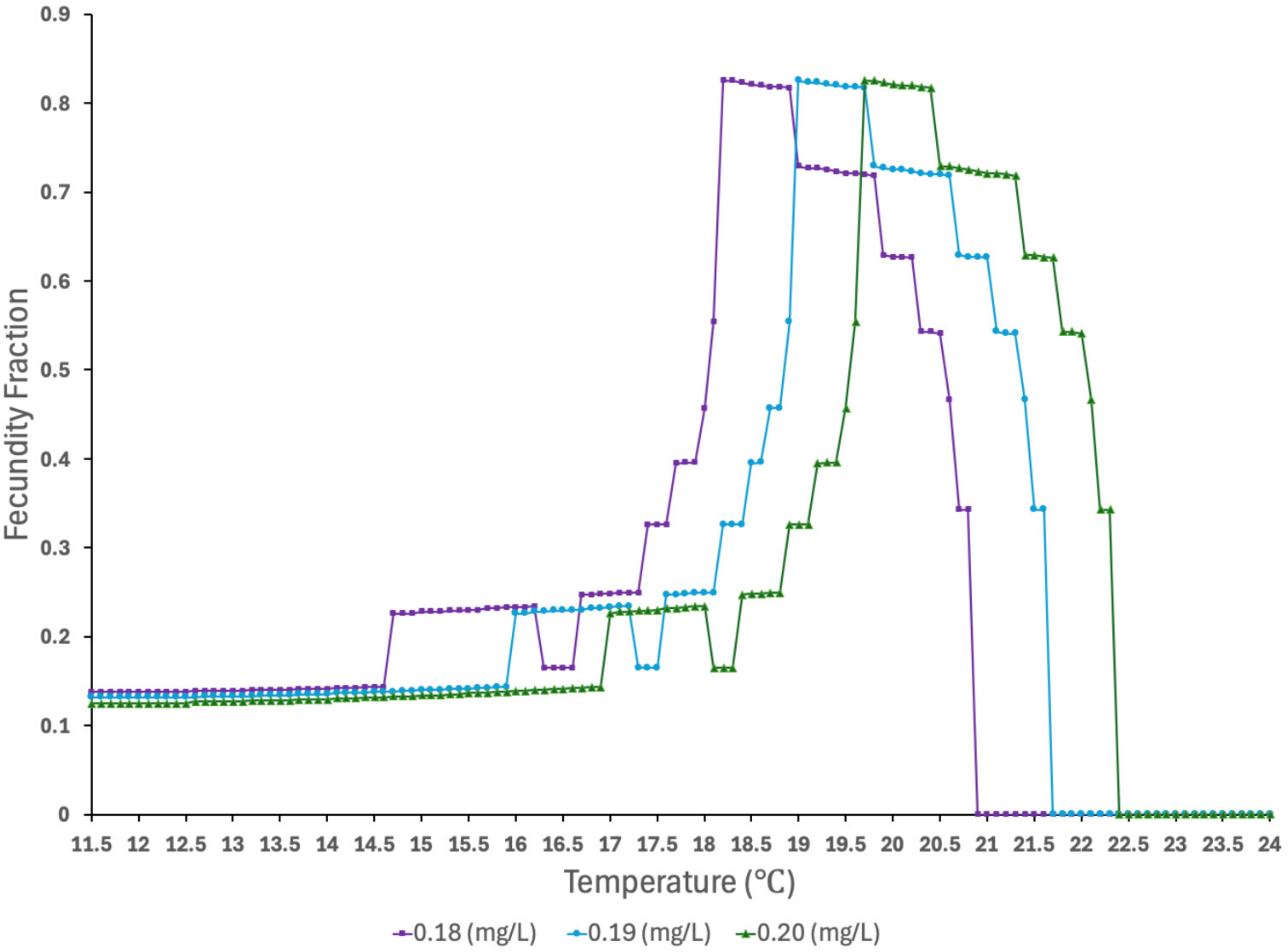

of the size limit, already constrained to a narrow range of temperatures, gradually becomes restricted to temperatures well above optimal, thus becoming inconsequential in determining the fecundity of the stock (Fig. 14). Thus, a size limit has primary influence under temperatures where physiological constraints already severely limit the contribution of the local population to the fecundity of the stock, minimizing any influence on stock population dynamics.

Spisula solidissima also lives in a region primarily characterized by a downcoast larval drift (Zhang et al. 2015, 2016), and hydrodynamics can influence regional recruitment (Czaja et al. 2023). Thus, for this species, a size limit influenced by a temperature restriction on maximum size also imposes its primary effect in a region inferred to be a sink, not a source, of larvae. Although not considered further here, details of connectivity certainly will influence the usefulness of a size limit imposed for purposes of sustainable management of any bivalve stock (Baskett et al. 2005; Munroe et al. 2013*b*, 2014; Alzate and Onstein 2022).

Conclusions

A temperature–size rule resulting in larger size at lower temperatures is well-described throughout the poikilotherm taxa, terrestrial, freshwater, and marine. Bivalves vary from the commonly accepted physiological basis in having size determined by ingestion and respiration rather than the dynamics of oxygen uptake and use. This physiology is well described, yet empirical support for a temperature–size rule is remarkably poorly documented. Herein is considered a prototypical large bivalve, *S. solidissima*, the size of which is large enough and the range extensive enough that identification of variations in size across geographic expanses should be readily obtained. A temperature–size relationship is identified for this species, first anticipated based on models of the species' physiology and second empirically; however, the clarity of the empirical evidence is strongly influenced by food supply, particularly under conditions when temperature permits a large maximum size. Likely, throughout the Bivalvia, food supply routinely imposes variations in size restricting detection of the temperature effect.

Spisula solidissima, like most species in the northwestern Atlantic, is shifting its range in response to rapidly warming temperatures. Considerations of the impact of this range shift on the species, the community, and the fishery must include a recognition that declining size on the trailing edge of the range is an expectation unless countered adventitiously by an increase in food supply. Size-dependent management measures will be impacted by this dynamic, with the physiological constraint on size likely limiting the effectiveness of any size limit expressed for biological purposes.

Models of range shift dynamics routinely examine changes in geographic occupation over time, and many address range boundary effects as a product of the dynamics of recruitment and mortality (e.g., Hughes et al. 2007; Garnier and Lewis 2016; Fredston-Hermann et al. 2020; Sirén and Morelli 2020). Herein is presented one more critical aspect of this population dynamics, the influence of changing temperature on the size–frequency distribution and regional productivity of the stock. For bivalves, such as *S. solidissima*, including consideration of the influence of temperature on demographics is an important piece of the range shift dynamics that deserves increased attention in biological models of and management responses to warming temperatures (Woodin et al. 2013; Mangano et al. 2020). To the extent that the primary influence on population dynamics most often will be concentrated at the trailing edge boundary, as is the case with *S. solidissima*, the influence of the temperature–size rule is likely to be primarily an issue of curtailment of landings by the fishery rather than provision of any substantive opportunity to develop regulatory options for sustainable management.

Acknowledgements

This research was supported by the National Science Foundation Industry/University Cooperative Research Center SCEMFIS (Science Center for Marine Fisheries) through membership fees under the direction of the Industry Advisory Board (IAB). SCEMFIS administrative support is provided by NSF awards #1841112, #1841435, #2332982, and #2332984. Conclusions and opinions expressed herein are solely those of the authors. The authors thank the NMFS Northeast Fisheries Science Center for making available the datasets used in this study.

Article information

History dates

Received: 5 December 2024
Accepted: 24 July 2025
Version of record online: 13 November 2025

Copyright

Data availability

All data used in this study were previously published or are available from the National Marine Fisheries Service-Northeast Fisheries Science Center and the website of the NSF Science Center for Marine Fisheries.

Author information

Author ORCIDs

Eric N. Powell https://orcid.org/0000-0001-9467-0248
Autumn L. Moya https://orcid.org/0000-0002-5300-9151
Daphne M. Munroe https://orcid.org/0000-0002-4388-7882
Roger Mann https://orcid.org/0000-0003-2001-8796
Sarah Borsetti https://orcid.org/0000-0002-3985-0294
Kelsey M. Kuykendall https://orcid.org/0000-0001-8931-1371

Author contributions

Conceptualization: ENP, RM
Data curation: ENP, ALM, DMM, RM, SB
Formal analysis: ENP, ALM, DMM, RM, SB
Funding acquisition: ENP
Investigation: ENP
Methodology: ENP, RM
Supervision: ENP
Writing – original draft: ENP, ALM, DMM, RM, SB
Writing – review & editing: ENP, ALM, DMM, RM, SB, KMK

Competing interests

No conflicts of interest exist.

References

Allen, J.A. 1877. The influence of physical conditions in the genesis of species. Radic. Rev. **1**: 108–140.

Allen, K.R. 1971. Relation between production and biomass. J. Fish. Res. Board Can. **28**: 1573–1581. doi:10.1139/f71-236.

Alzate, A., and Onstein, R.E. 2022. Understanding the relationship between dispersal and range size. Ecol. Lett. **25**: 2303–2323. doi:10.1111/ele.14089.

Amaya, D.J., Jacox, M.G., Alexander, M.A., Scott, J.D., Deser, C., Capotondi, A., and Phillips, A.S. 2023. Bottom marine heatwaves along the continental shelves of North America. Nat. Commun. **14**: 1038. doi:10.1038/s41467-023-36567-0.

Andrews, K.I., and Mangel, M. 2012. Asymptotic size and natural mortality of long-lived fish for data poor stock assessments. Fish. Res. **127–128**: 45–48. doi:10.1016/j.fishres.2012.04.005.

Atkinson, D. 1994. Temperature and organism size—a biological law for ectotherms. Adv. Ecol. Res. **25**: 1–58.

Audzijonyte, A., Jakubavičiūtė, E., Lindmark, M., and Richards, A.A. 2022. Mechanistic temperature-size rule explanation should reconcile physiological and mortality responses to temperature. Biol. Bull. **243**: 220–238. doi:10.1086/722027.

Bald, J., Sinquin, A., Borja, A., Caill-Milly, N., Duclercq, B., Dang, C., and de Montaundouin, X. 2009. A system dynamics model for the management of the Manila clam, *Ruditapes philippinarum* (Adams and Reeve, 1850) in the Bay of Arcachon (France). Ecol. Modell. **220**: 2828–2837. doi:10.1016/j.ecolmodel.2009.03.031.

Barber, B.J., Ford, S.E., and Wargo, R.N. 1991. Genetic variation in the timing of gonadal maturation and spawning of the Eastern oyster, *Crassostrea virginica* Gmelin. Biol. Bull. **181**: 216–221. doi:10.2307/1542092.

Baskett, M.L., Levin, S.A., Gaines, S.D., and Dushoff, J. 2005. Marine reserve design and the evolution of size at maturation in harvested fish. Ecol. Appl. **15**: 882–901. doi:10.1890/04-0723.

Bauer, G. 1992. Variation in the life span and size of the freshwater pearl mussel. J. Anim. Ecol. **61**: 425–436. doi:10.2307/5333.

Bayne, B.L. 2001. Comment: physiological regulation versus autonomous filtration in filter-feeding bivalves: starting points for progress. Reply to comment by H.U. Riisgård. Ophelia, **54**: 211. doi:10.1080/00785236.2001.10409466.

Bell, G. 1980. The costs of reproduction and their consequences. Am. Nat. **116**: 45–76. doi:10.1086/283611.

Bergmann, C. 1847. Ueber die verhältnisse der wärmeökonomie der Thiere zu ihrer Grösse. Göttinger Studien, **1**: 595–708.

Berke, S.K., Jablonski, E., Krug, A.Z., Roy, K., and Tomašových, A. 2013. Beyond Bergmann's rule: size-latitude relationships in marine *Bivalvia* world-wide. Global Ecol. Biogeogr. **22**: 173–183. doi:10.1111/j.1466-8238.2012.00775.x.

Berrigan, M., Candies, T., Cirino, J., Dugas, R., Dyer, C., Gray, J., et al. 1991. The oyster fishery of the Gulf of Mexico, United States: a regional management plan. Gulf States Marine Fisheries Commission, No. 24, Ocean Springs, Mississippi.

Beukema, J.J., and Dekker, R. 2019. The carrying capacity of a tidal flat area for suspension-feeding bivalves. Mar. Ecol. Prog. Ser. **629**: 55–65. doi:10.3354/meps13099.

Beukema, J.J., Dekker, R., Drent, J., and van der Meer, J. 2017. Long-term changes in annual growth of bivalves in the Wadden Sea: influences of temperature, food, and abundance. Mar. Ecol. Prog. Ser. **573**: 143–156. doi:10.3354/meps12122.

Borges, L., Zuur, A.F., Ragan, E., and Officer, K. 2006. Modelling discard ogives from Irish demersal fisheries. ICES J. Mar. Sci. **63**: 1086–1095. doi:10.1016/j.icesjms.2006.03.017.

Borsetti, S., Hollyman, P.R., and Munroe, D. 2021. Using a sclerochronological approach to determine a climate-growth relationship for waved whelk, *Buccinum undatum*, in the U.S. Mid-Atlantic. Estuarine Coastal Shelf Sci. **252**: 107255. doi:10.1016/j.ecss.2021.107255.

Borsetti, S., Munroe, D., Rudders, D., Dobson, C., and Bochenek, E. 2018. Spatial variation in life history characteristics of waved whelk (*Buccinum undatum* L.) on the U.S. Mid-Atlantic continental shelf. Fish. Res. **198**: 129–137. doi:10.1016/j.fishres.2017.10.006.

Brey, T., and Gage, J.E. 1997. Interactions of growth and mortality in benthic invertebrate populations: empirical evidence for a mortality-growth continuum. Arch. Fish. Mar. Res. **45**: 45–59.

Brody, S. 1945. Bioenergetics and growth, with special reference to the efficiency complex in domestic animals. Reinhold Publishing Corporation, New York.

Brody, S., Ragsdale, A.C., and Turner, C.W. 1923. The rate of growth of the dairy cow II. Growth in weight after the age of two years. J. Gen. Physiol. **5**: 445–449. doi:10.1085/jgp.5.4.445.

Buxton, C.D., Newell, R.C., and Field, J.G. 1981. Response-surface analysis of the combined effects of exposure and acclimation temperature on filtration, oxygen consumption and scope for growth in the oyster *Ostrea edulis*. Mar. Ecol. Prog. Ser. **6**: 73–82. doi:10.3354/meps006073.

Calow, P. 1977. Conversion efficiencies in heterotrophic organisms. Biol. Rev. **52**: 385–409. doi:10.1111/j.1469-185X.1977.tb00840.x.

Cardoso, J.F.M.F., Peralto, N.R.E., Machado, J.P., and van der Veer, H.W. 2013. Growth and reproductive investment of introduced Pacific oysters *Crassostrea gigas* in southern European waters. Estuarine Coastal Shelf Sci. **118**: 24–30. doi:10.1016/j.ecss.2012.12.017.

Charnov, E.L., Warne, R., and Moses, M. 2007. Lifetime reproductive effort. Am. Nat. **170**: E129–E142. doi:10.1086/522840.

Chen, Z., Curchitser, E., Chant, R., and Kang, D. 2018. Seasonal variability of the Cold Pool over the Mid-Atlantic Bight continental shelf. J. Geophys. Res.: Oceans, **123**: 8203–8226. doi:10.1029/2018JC014148.

Chintala, M.M., and Grassle, J.P. 1995. Early gametogenesis and spawning in "juvenile" Atlantic surfclam, *Spisula solidissima* (Dillwyn, 1819). J. Shellfish Res. **14**: 301–306.

Chintala, M.M., and Grassle, J.P. 2001. Comparison of recruitment frequency and growth of surfclams, *Spisula solidissima* (Dillwyn, 1817), in different inner-shelf habitats of New Jersey. J. Shellfish Res. **20**: 1177–1186.

Choi, K.S., Powell, E.N., Lewis, D.H., and Ray, S.M. 1994. Instantaneous reproductive effort in female American oysters, *Crassostrea virginica*, measured by a new immunoprecipitation assay. Biol. Bull. **186**: 41–61. doi:10.2307/1542035.

Chute, A.S., McBride, R.S., Emery, S.J., and Robillard, E. 2016. Annulus formation and growth of Atlantic surfclam (*Spisula solidissima*) along a latitudinal gradient in the western North Atlantic Ocean. J. Shellfish Res. **35**: 729–737. doi:10.2983/035.035.0402.

Coggins, L.G., Jr., Catalano, M.J., Allen, M.S., Pine, W.E., III, and Walters, C.J. 2007. Effects of cryptic mortality and the hidden costs of using length limits in fishery management. Fish Fish. **8**: 196–210. doi:10.1111/j.1467-2679.2007.00247.x.

Cognie, B., Barillé, L., and Rincé, Y. 2001. Selective feeding of the oyster *Crassostrea gigas* fed on a natural microphytobenthos assemblage. Estuaries, **24**: 126–131. doi:10.2307/1352819.

Czaja, R., Jr., Hennen, D., Cerrato, R., Lwiza, K., Pales-Espinosa, E., O'Dwyer, J., and Using, A.B. 2023. LASSO regularization to project recruitment under CMIP6 climate scenarios in a coastal fishery with spatial oceanographic gradients. Can. J. Fish. Aquat. Sci. **80**: 1032–1046. doi:10.1139/cjfas-2022-0091.

Diaz, M.G., Hofmann, E.E., Klinck, J.M., Munroe, D.M., Powell, E.N., and Scheld, A.M. 2024. Spatial and temporal variability of Atlantic surfclam (*Spisula solidissima*, Dillwyn 1817) population demographics along the Middle Atlantic Bight. J. Shellfish Res. **43**: 37–49. doi:10.2983/035.043.0104.

Du Pontavice, H., Chen, Z., and Saba, V.S. 2023. A high-resolution ocean bottom temperature product for the northeast U.S. continental shelf marine ecosystem. Prog. Oceanogr. **210**: 102948. doi:10.1016/j.pocean.2022.102948.

DuBose, T.P., Patten, M.A., Holt, A.S., and Vaughn, C.C. 2022. Latitudinal variation in freshwater mussel potential maximum length in eastern North America. Freshw. Biol. **67**: 1020–1034. doi:10.1111/fwb.13898.

Dye, A.H. 1979. The effect of acute and longterm temperature changes on the respiration of two sand-dwelling bivalves. Comp. Biochem. Physiol. A Physiol. **63**: 405–409. doi:10.1016/0300-9629(79)90611-X.

Ehrich, M.K., and Harris, L.A. 2015. A review of existing eastern oyster filtration rate models. Ecol. Modell. **297**: 201–212. doi:10.1016/j.ecolmodel.2014.11.023.

Eierman, L.E., and Hare, M.P. 2016. Reef-specific patterns of gene expression plasticity in eastern oysters (*Crassostrea virginica*). J. Hered. **107**: 90–100. doi:10.1093/jhered/esv057.

Evans, S., and Langdon, C. 2006a. Direct and indirect responses to selection on individual body weight in the Pacific oyster (*Crassostrea gigas*). Aquaculture, **261**: 546–555. doi:10.1016/j.aquaculture.2006.07.037.

Evans, S., and Langdon, C. 2006b. Effects of genotype × environment interactions on the selection of broadly adapted Pacific oysters (*Crassostrea gigas*). Aquaculture, **261**: 522–534. doi:10.1016/j.aquaculture.2006.07.022.

Fay, C.W., Neves, R.J., and Pardue, G.B. 1983. Species profiles: life histories and environmental requirements of coastal fishes and invertebrates (Mid-Atlantic): surfclam. Fish and Wildlife Service FWS/OBS-82/11/13, United States Department of Interior, Washington, D.C.

Flye-Sainte-Marie, J., Jean, F., Paillard, C., Ford, S., Powell, E., Hofmann, E., and Klinck, J. 2007. Ecophysiological dynamic model of individual growth of *Ruditapes philippinarum*. Aquaculture, **266**: 130–143. doi:10.1016/j.aquaculture.2007.02.017.

Forster, J., and Hirst, A.G. 2012. The temperature-size rule emerges from ontogenetic differences between growth and development rates. Funct. Ecol. **26**: 483–492. doi:10.1111/j.1365-2435.2011.01958.x.

Forster, J., Hirst, A.G., and Atkinson, D. 2012. Warming induced reductions in body size are greater in aquatic than terrestrial species. Proc. Natl. Acad. Sci. **109**: 19310–19314. doi:10.1073/pnas.1210460109.

Frechette, M, and Lefaivre, D. 1990. Discriminating between food and space limitation in benthic suspension feeders using self-thinning relationships. Mar. Ecol. Prog. Ser. **65**: 15–23. doi:10.3354/meps065015.

Fredston-Hermann, A., Selden, R., Pinsky, M., Gaines, S.D., and Halpern, B.S. 2020. Cold range edges of marine fishes track climate change better than warm edges. Global Change Biol. **26**: 2908–2922. doi:10.1111/gcb.15035.

Freitas, V., Cardoso, J.F.M.F., Santos, S., Campos, J., Drent, J., Saraiva, S., et al. 2009. Reconstruction of food conditions for northeast Atlantic bivalve species based on dynamic energy budgets. J. Sea Res. **62**: 75–82. doi:10.1016/j.seares.2009.07.004.

Friedland, K.D., Miles, T., Goode, A.G., Powell, E.N., and Brady, D.C. 2022. The Middle Atlantic Bight Cold Pool is warming and shrinking: indices from in situ autumn seafloor temperatures. Fish. Oceanogr. **31**: 217–223. doi:10.1111/fog.12573.

Friedland, K.D., Morse, R.E., Manning, J.P., Melrose, D.C., Miles, T., Goode, A.G., et al. 2020. Trends and change points in surface and bottom thermal environments of the US northeast continental shelf ecosystem. Fish. Oceanogr. **29**: 396–414. doi:10.1111/fog.12485.

Garnier, J., and Lewis, M.A. 2016. Expansion under climate change: the genetic consequences. Bull. Math. Biol. **78**: 2165–2185. doi:10.1007/s11538-016-0213-x.

Getz, W.M. 2011. Biomass transformation webs provide a unified approach to consumer resource modelling. Ecol. Lett. **14**: 113–124. doi:10.1111/j.1461-0248.2010.01566.x.

Gray, J. 1928. The growth of fish III. The effect of temperature on the development of the eggs of *Salmo fario*. J. Exp. Biol. **6**: 125–130. doi:10.1242/jeb.6.2.125.

Hale, S.S. 2010. Biogeographical patterns of marine benthic macroinvertebrates along the Atlantic coast of the northeastern USA. Estuaries Coasts, **33**: 1039–1053. doi:10.1007/s12237-010-9332-z.

Hallam, A. 1965. Environmental causes of stunting in living and fossil marine benthonic invertebrates. Palaeontology, **8**: 132–155.

Hancock, D.A. 1973. The relationship between stock and recruitment in exploited invertebrates. Rapports et Procès-verbaux des Réunions, Conseil International pour l'Exploration de la Mer, **164**: 113–131.

Harford, W.J., Dowling, N.A., Prince, J.D., Hurd, F., Bellquist, L., Likins, J., and Wilson, J.R. 2019. An indicator-based decision framework for the northern California red abalone fishery. Ecosphere, **10**(1): e02533. doi:10.1002/ecs2.2533.

Hart, D.R., and Chute, A.S. 2009. Estimating von Bertalanffy growth parameters from growth increment data using a linear mixed-effects model, with an application to the sea scallop *Placopecten magellanicus*. ICES J. Mar. Sci. **66**: 2165–2175. doi:10.1093/icesjms/fsp188.

Hemeon, K.M., Ashton-Alcox, K.A., Powell, E.N., Pace, S.M., Poussard, L.M., Solinger, L.K., and Soniat, T.M. 2020. Novel shell stock-recruitment models for *Crassostrea virginica* as a function of regional shell effective surface area, missing link for sustainable management. J. Shellfish Res. **39**: 633–654. doi:10.2983/035.039.0310.

Henderson, I.M. 2009. Optimising recreational harvests of blue cod: the effects of catch-and-release mortality and size selectivity. Fish. Res. **99**: 184–195. doi:10.1016/j.fishres.2009.06.003.

Hennen, D.R., Mann, R., Munroe, E.M., and Powell, E.N. 2018. Biological reference points for Atlantic surfclam (*Spisula solidissima*) in warming seas. Fish. Res. **207**: 126–139. doi:10.1016/j.fishres.2018.06.013.

Hochwald, S. 2001. Plasticity of life-history traits in *Unio crassus*. *In* Ecology and evolution of the freshwater mussels Unionida. Vol. 145. *Edited by* G. Bauer and E. Wächtler. Ecological Studies. Springer-Verlag. pp. 127–141. doi:10.1007/978-3-642-56869-5_7.

Hoenig, J.M. 1983. Empirical use of longevity data to estimate mortality rates. Fish. Bull. **83**: 898–903.

Hofmann, E.E., Klinck, J.M., Kraeuter, J.N., Powell, E.N., Grizzle, R.E., Buckner, S.C., and Bricelj, V.M. 2006. A population dynamics model of the hard clam, *Mercenaria mercenaria*: development of the age- and length-frequency structure of the population. J. Shellfish Res. **25**: 417–444. doi:10.2983/0730-8000(2006)25[417:APDMOT]2.0.CO;2.

Hofmann, E.E., Powell, E.N., Klinck, J.M., Munroe, D.M., Mann, R., Haidvogel, D.B. et al. 2018. An overview of factors affecting distribution of the Atlantic surfclam (Spisula solidissima), a continental shelf biomass dominant, during a period of climate change. J. Shellfish Res. **37**: 821–831. doi:10.2083/035.037.0412

Holland, A., and Dean, J. 1977. The biology of the stout razor clam Tagelus plebeius: I. Animal-sediment relationships, feeding mechanism, and community biology. Ches. Sci. **18**: 58–66. doi:10.2307/1350364.

Honkoop, P.J.C., and Bayne, B.L. 2002. Stocking density and growth of the Pacific oyster (*Crassostrea gigas*) and the Sydney rock oyster (*Saccostrea glomerata*) in Port Stephens, Australia. Aquaculture, **213**: 171–186. doi:10.1016/S0044-8486(02)00030-3.

Hughes, A.R., Hanley, T.C., Byers, J.E., Grabowski, J.H., McCrudden, T., Piehler, M.F., and Kimbro, D.L. 2019. Genetic diversity and phenotype variation within hatchery-produced oyster cohorts predict size and success in the field. Ecol. Appl. **29**: e01940. doi:10.1002/eap.1940.

Hughes, C.L., Dytham, C., and Hill, J.K. 2007. Modelling and analysing evolution of dispersal in populations at expanding range boundaries. Ecol. Entomol. **32**: 437–445. doi:10.1111/j.1365-2311.2007.00890.x.

Irie, T., Morimoto, N., and Fischer, K. 2013. Higher calcification costs at lower temperatures do not break the temperature-size rule in an intertidal gastropod with determinate growth. Mar. Biol. **160**: 2619–2629. doi:10.1007/s00227-013-2256-y.

Jacobson, L.D., and Hennen, D.R. 2019. Improving the NEFSC clam survey for Atlantic surfclams and ocean quahogs. Northeast Fish. Sci. Center Ref. Doc. **19–06**: 85. doi:10.25923/745e-3g62.

James, F.C. 1970. Geographic size variation in birds and its relationship to climate. Ecology, **51**: 365–390. doi:10.2307/1935374.

Jensen, A.L. 1997. Origin of the relation between *K* and *L* and synthesis of relations among life history parameters. Can. J. Fish. Aquat.Sci. **54**: 987–989. doi:10.1139/f97-007.

John, C.C. 1933. Effects of temperature on the determination of size of species. Curr. Sci. **1**: 189–191.

Jones, D.S. 1981. Reproductive cycles of the Atlantic surfclam *Spisula solidissima*, and the ocean quahog *Arctica islandica* off New Jersey. J. Shellfish Res. **1**: 23–32.

Jørgensen, C.B., Møhlenberg, F., and Stenknudsen, O. 1986. Nature of the relation between ventilation and oxygen consumption in filter feeders. Mar. Ecol. Prog. Ser. **29**: 73–88.

Kang, S.G., Choi, K.S., Bulgakov, A.A., Kim, Y., and Kim, S.Y. 2003. Enzyme-linked immunosorbent assay (ELISA) used in quantification of reproductive capacity in the Pacific oyster, *Crassostrea gigas*, in Korea. J. Exp. Mar. Biol. Ecol. **282**: 1–21. doi:10.1016/S0022-0981(02)00444-6.

Keohane, I.P., Tay, J., Gawde, R.K., and Hood, R.R. 2019. Sensitivity of a biogeochemical model to the formulation of oyster filtration. Ecol. Modell. **403**: 70–84. doi:10.1016/j.ecolmodel.2019.04.003.

Kessler, A., Goris, N., and Lauvset, S.K. 2022. Observation-based sea surface temperature trends in Atlantic large marine ecosystems. Prog. Oceanogr. **208**: 102902. doi:10.1016/j.pocean.2022.102902.

Kilada, R.W., Campana, S.E., and Roddick, D. 2009. Growth and sexual maturity of the northern propellerclam (*Cyrtodaria siliqua*) in eastern Canada, with bomb radiocarbon age validation. Mar. Biol. **156**: 1029–1037. doi:10.1007/s00227-009-1146-9.

Kim, Y., and Powell, E.N. 2004. Surfclam histopathology survey along the Delmarva mortality line. J. Shellfish Res. **23**: 429–441.

Klinck, J.M., Powell, E.N., Hemeon, K.M., Sower, J.R., and Hennen, D.R. 2023. A growth model for *Arctica islandica*: the performance of Tanaka and the temptation of von Bertalanffy—can the two coexist? J. Shellfish Res. **42**: 77–90. doi:10.2983/035.042.0108.

Kraeuter, J.N., Buckner, S., and Powell, E.N. 2005. A note on a spawner-recruit relationship for a heavily exploited bivalve: the case of northern quahog (hard clams), *Mercenaria mercenaria* in Great South Bay New York. J. Shellfish Res. **24**: 1043–1052. doi:10.2983/0730-8000(2005)24[1043:ANOASR]2.0.CO;2.

Kraeuter, J.N., Klinck, J.M., Powell, E.N., Hofmann, E.E., Buckner, S.C., Grizzle, R.W., and Bricelj, V.M. 2008. Effects of the fishery on the northern quahog (=hard clam, *Mercenaria mercenaria* L.) population in Great South Bay, New York: a modeling study. J. Shellfish Res. **27**: 653–666. doi:10.2983/0730-8000(2008)27[653:EOTFOT]2.0.CO;2.

Langdon, C., Evans, F., Jacobson, D., and Blouin, M. 2003. Yields of cultured Pacific oysters *Crassostrea gigas* Thunberg improved after one generation of selection. Aquaculture, **220**: 227–244. doi:10.1016/S0044-8486(02)00621-X.

Lavin, C.P., Gordó-Vilaseca, C., Costello, M.J., Shi, Z.Y., Stephenson, F., and Gruss, A. 2022. Warm and cold temperatures limit the maximum body length of teleost fishes across a latitudinal gradient in Norwegian waters. Environ. Biol. Fishes, **105**: 1415–1429. doi:10.1007/s10641-022-01270-4.

Le, D.V., Alfaro, A.C., Ibarrola, I., Ragg, N.L.C., Hilton, Z., and King, N. 2017. Allometric scaling of physiological rates in the New Zealand geoduck clam, *Panopea zelandica*. Aquaculture, **473**: 105–109. doi:10.1016/j.aquaculture.2017.02.001.

LeClaire, A.M., Powell, E.N., Mann, R., Hemeon, K.M., Pace, S.M., Saba, V., et al. 2024. Temporal and spatial comparisons of ocean quahog (*Arctica islandica*) growth and lifespan on the mid-Atlantic continental shelf during inshore transgressions of their range from the neoglacial through the twentieth century. Cont. Shelf Res. **272**: 105143. doi:10.1016/j.csr.2023.105143.

Ledoux, T., Clements, J.C., Maillet, M., Gallant, D., Sonier, R., and Miron, G. 2023. Reproductive ecology of the soft-shell clam (*Mya arenaria*) in Eastern New Brunswick, Canada: assessing size-at-maturity and spawning time to inform fisheries management. Fish. Res. **265**: 106759. doi:10.1016/j.fishres.2023.106759.

Lomovasky, B., Baldoni, A., Ribeiro, P., Alvarez, G., Lasta, M., Campodónico, S., and Iribarne, O. 2011. Exploring the causes of differences in growth rate of the Patagonian scallop *Zygochlamys patagonica* along its commerical bed distribution in the SW Atlantic. J. Sea Res. **66**: 162–171. doi:10.1016/j.seares.2011.05.010.

Lucey, S.M., and Nye, J.A. 2010. Shifting species assemblages in the northeast US continental shelf large marine ecosystem. Mar. Ecol. Prog. Ser. **415**: 23–33. doi:10.3354/meps08743.

Ma, H., Grassle, J.P., and Rosario, J.M. 2006. Initial recruitment and growth of surfclams (*Spisula solidissima* Dillwyn) on the inner continental shelf of New Jersey. J. Shellfish Res. **25**: 481–489. doi:10.2983/0730-8000(2006)25[481:IRAGOS]2.0.CO;2.

Mancera, E., and Mendo, J. 1996. Population dynamics of the oyster *Crassostrea rhizophorae* from the Ciénaga Grande de Santa Marta, Colombia. Fish. Res. **26**: 139–148. doi:10.1016/0165-7836(95)00401-7.

Mangano, M.C., Mieszkowska, N., Helmuth, B., Domingos, T., Sousa, T., Baiamonte, G., et al. 2020. Moving toward a strategy for addressing climate displacement of marine resources: a proof-of-concept. Front. Mar. Sci. **7**: 408. doi:10.3389/fmars.2020.00408.

Männer, L., Mundinger, C., and Haase, M. 2022. Stay in shape: assessing the adaptive potential of shell morphology and its sensitivity to temperature in the invasive New Zealand mud snail through phenotypic plasticity and natural selection in Europe. Ecol. Evol. **12**: e9314. doi:10.1002/ece3.9314.

Martinez del Rio, C., and Karasov, W.H. 2010. Body size and temperature: why they matter. Nat. Educ. Knowl. **3**(10): 10.

Marzec, R.J., Kim, Y., and Powell, E.N. 2010. Geographic trends in weight and condition index of surfclams (*Spisula solidissima*) in the Mid-Atlantic Bight. J. Shellfish Res. **29**: 117–128. doi:10.2983/035.029.0104.

McCarty, A.J., McFarland, K., Small, J., Allen, S.K., Jr., and Plough, L.V. 2020. Heritability of acute low salinity survival in the Eastern oyster, (*Crassostrea virginica*). Aquaculture, **529**: 735649. doi:10.1016/j.aquaculture.2020.735649.

McCay, B.J., Brandt, S., and Creed, C.F. 2011. Human dimensions of climate change and fisheries in a coupled system: the Atlantic surfclam case. ICES J. Mar. Sci. **68**: 1354–1367. doi:10.1093/icesjms/fsr044.

McIntyre, R., Lawler, A., and Masefield, R. 2015. Size of maturity of the common whelk, *Buccinum undatum*: is the minimum landing size in England too low? Fish. Res. **162**: 53–57. doi:10.1016/j.fishres.2014.10.003.

McQueen, A., Klaassen, M., Tattersall, G.J., Atkinson, R., Jessop, R., Hassell, C.J., and Christie, M., Victorian Water Study Group, Australian Wader Studies Group and Symonds, M.R.E. 2022. Thermal adaptation best explains Bergmann's and Allen's Rules across ecologically diverse shorebirds. Nat. Commun. **13**: 4727. doi:10.1038/s41467-022-32108-3.

Mills, K.E., Kemberling, A., Kerr, L.A., Lucey, S.M., McBride, R.S., Nye, J.A., et al. 2024. Multispecies population-scale emergence of climate change signals in an ocean warming hotspot. ICES J. Mar. Sci. **81**: 375–389. doi:10.1093/icesjms/fsad208.

Montalto, V., Rinaldi, A., and Sarà, G. 2015. Life history traits to predict biogeographic species distributions in bivalves. Sci. Nat. **102**: 61. doi:10.1007/s00114-015-1313-4.

Moore, J.L., Lipcius, R.N., Puckett, B., and Schreiber, S.J. 2016. The demographic consequence of growing older and bigger in oyster populations. Ecol. Appl. **26**: 2206–2217. doi:10.1002/eap.1374.

Moss, D.K., Ivany, J.C., Judd, E.J., Cummings, P.W., Bearden, C.E., Kim, W.-J., et al. 2016. Lifespan, growth rate, and body size across latitude in marine Bivalvia, with implications for Phanerozoic evolution. Proc. R Soc. B Biol. Sci. **283**: 20161364. doi:10.1098/rspb.2016.1364.

Mouw, C.B., and Yoder, J.A. 2005. Primary production calculations in the Mid-Atlantic Bight including effects of phytoplankton community size structure. Limnol. Oceanogr. **50**: 1232–1243. doi:10.4319/lo.2005.50.4.1232.

Mugabe, E.D., Amoda, C.A., and Griffiths, C.L. 2019. Population structure and growth of the beaked clam *Eumarcia poupercula* (Bivalvia, Veneridae) in Maputo Bay, Mozambique. Afr. J. Mar. Sci. **41**: 385–393. doi:10.2989/1814232X.2019.1679255.

Munroe, D.M., Haidvogel, D., Caracappa, J.C., Klinck, J.M., Powell, E.N., Hofmann, E.E., et al. 2018. Modeling larval dispersal and connectivity for Atlantic sea scallop (*Placopecten magellanicus*) in the Middle Atlantic Bight. Fish. Res. **208**: 7–15. doi:10.1016/j.fishres.2018.06.020.

Munroe, D.M., Hofmann, E.E., Powell, E.N., and Klinck, J.M. 2013b. How do shellfisheries influence genetic connectivity in metapopulations? A modeling study examining the role of lower size limits in oyster fisheries. Can. J. Fish. Aquat. Sci. **70**: 1813–1828. doi:10.1139/cjfas-2013-0089.

Munroe, D.M., Klinck, J.M., Hofmann, E.E., and Powell, E.N. 2014. A modelling study of the role of marine protected areas in metapopulation genetic connectivity in Delaware Bay oysters. Aquat. Conserv.: Mar. Freshw. Ecosyst. **24**: 645–666. doi:10.1002/aqc.2400.

Munroe, D.M., Narváez, D.A., Hennen, D., Jacobson, L., Mann, R., Hofmann, E.E., et al. 2016. Fishing and bottom water temperature as drivers of change in maximum shell length in Atlantic surfclams (*Spisula solidissima*). Estuarine Coastal Shelf Sci. **170**: 112–122. doi:10.1016/j.ecss.2016.01.009.

Munroe, D.M., Powell, E.N., Ford, S.E., Hofmann, E.E., and Klinck, J.M. 2015. Outcomes of asymmetric selection pressure and larval dispersal on evolution of disease resistance: a metapopulation modeling study with oysters. Mar. Ecol. Prog. Ser. **531**: 221–239. doi:10.3354/meps11349.

Munroe, D.M., Powell, E.N., Klinck, J.M., Scheld, A.M., Borsetti, S., Beckensteiner, J., and Hofmann, E.E. 2022. The Atlantic surfclam fishery and offshore wind energy development: 1. Model development and verification. ICES J. Mar. Sci. **79**: 1787–1800. doi:10.1093/icesjms/fsac108.

Munroe, D.M., Powell, E.N., Mann, R., Klinck, J.M., and Hofmann, E.E. 2013a. Underestimation of primary productivity on continental shelves: evidence from maximum size of extant surfclam (*Spisula solidissima*) populations. Fish. Oceanogr. **22**: 220–233. doi:10.1111/fog.12016.

Narváez, D.A., Munroe, D.M., Hofmann, E.E., Klinck, J.M., Powell, E.N., Mann, R., and Curchitser, E. 2015. Long-term dynamics in Atlantic surfclam (*Spisula solidissima*) populations: the role of bottom water temperature. J. Mar. Syst. **141**: 136–148. doi:10.1016/j.jmarsys.2014.08.007.

Nawrot, R., Albano, P.G., Chattopadhyay, D., and Zuschin, M. 2017. Climate change and body size shift in Mediterranean bivalve assemblages: unexpected role of biological invasions. Proc. R Soc. B Biol. Sci. **284**: 20170357. doi:10.1098/rspb.2017.0357.

NEFSC (Northeast Fisheries Science Center) 2007. 44th Northeast Regional Stock Assessment Workshop (44th SAW) assessment report. Northeast Fisheries Science Center Reference Document, **07–10**: 661.

NEFSC (Northeast Fisheries Science Center) 2017. 61st Northeast Regional Stock Assessment Workshop (61st SAW) Assessment report. Northeast Fish. Sci. Cent. Ref. Doc. **17–05**: 464.

NEFSC (Northeast Fisheries Science Center), 2022. Management track assessments completed in Spring 2020. Northeast Fish. Sci. Cent. Ref. Doc. **22–09**: 86.

Neuman, M. 1996. Evidence of upwelling along the New Jersey coastline and the south shore of Long Island, New York. Bull. New Jersey Acad. Sci. **41**: 7–13.

Nicol, D. 1964. An essay on size of marine pelecypods. J. Paleontol. **38**: 968–974.

Nicol, D. 1978. Size trends in living pelecypods and gastropods with calcareous shells. Nautilus, **92**: 70–79.

Ohnishi, S., Yamakawa, T., Okamura, H., and Akamine, T. 2012. A note on the von Bertalanffy growth function concerning the allocation of surplus energy to reproduction. Fish. Bull. **110**: 213–229.

Ólafsson, E.B., Peterson, C.H., and Ambrose, W.G., Jr. 1994. Does recruitment limitation structure populations and communities of macro-invertebrates in marine soft sediments: the relative significance of pre- and post-settlement processes. Oceanogr. Mar. Biol.: Ann. Rev. **32**: 65–109.

Pauly, D., Amarasinghe, U.S., Chu, E., Freire, K.M.F., Vazquez, E., and Butler, M.J., IV 2022. The growth, respiration, and reproduction of crustaceans: a synthesis through the Gill-Oxygen Limitation theory (GOLT). J. Crustac. Biol. **42**: 1–13. doi:10.1093/jcbiol/ruac059.

Perretti, C.T., Fogarty, M.J., Friedland, K.D., Hare, J.A., Lucey, S.M., McBride, R.S., et al. 2017. Regime shifts in fish recruitment on the northeast U.S. continental shelf. Mar. Ecol. Prog. Ser. **574**: 1–11. doi:10.3354/meps12183.

Pershing, A.J., Alexander, M.A., Brady, D.C., Brickman, D., Curchitser, E.N., Diamond, A.W., et al. 2021. Climate impacts on the Gulf of

Maine ecosystem: a review of observed and expected changes in 2050 from rising temperatures. Elementa: Sci. Anthropocene, **9**(1): p.elementa2020.00076. doi:10.1525/elementa.2020.00076.

Pershing, A.J., Alexander, M.A., Hernandez, C.M., Kerr, L.A., le Bris, A., Mills, K.E., et al. 2015. Slow adaptation in the face of rapid warming leads to collapse of the Gulf of Maine cod fishery. Science, **350**: 809–812. doi:10.1126/science.aac9819.

Peterson, C.H. 2002. Recruitment overfishing in a bivalve mollusc fishery: hard clams (*Mercenaria mercenaria*) in North Carolina. Can. J. Fish. Aquat.Sci. **59**: 96–104. doi:10.1139/f01-196.

Peterson, C.H., and Summerson, H.C. 1992. Basin-scale coherences of population dynamics of an exploited marine invertebrate, the bay scallop: implications of recruitment limitation. Mar. Ecol. Prog. Ser. **90**: 257–272. doi:10.3354/meps090257.

Phelps, H.L. 1994. The Asiatic clam (*Corbicula fluminea*) invasion and system-level ecological change in the Potomac River Estuary near Washington, D.C. Estuaries, **17**: 614–621. doi:10.2307/1352409.

Pousse, E., Munroe, D., Hart, D., Hennen, D., Cameron, L.P., Rheuban, J.E., et al. 2021. Dynamic energy budget modeling of Atlantic surfclam, *Spisula solidissima*, under future ocean acidification and warming. Mar. Environ. Res. **177**: 105602. doi:10.1016/j.marenvres.2022.105602.

Powell, E.N., and Stanton, R.J., Jr. 1985. Estimating biomass and energy flow of molluscs in paleo-communities. Palaeontology, **28**: 1–34.

Powell, E.N., Bochenek, E.A., and DePersenaire, J. 2010. Evaluation of bag-and-size-limit options in the management of summer flounder *Paralichthys dentatus*. Fish. Res. **105**: 215–227. doi:10.1016/j.fishres.2010.05.011.

Powell, E.N., Bochenek, E.A., DePersenaire, J., and King, S.E. 2011. Injury frequency for discarded summer flounder in the recreational fishery of the Mid-Atlantic Bight: influence of landing size regulations. Am. Fish. Soc. Symp. **75**: 171–187.

Powell, E.N., Ewing, A.M., and Kuykendall, K.M. 2020a. Ocean quahogs (*Arctica islandica*) and Atlantic surfclams (*Spisula solidissima*) on the Mid-Atlantic Bight continental shelf and Georges Bank: the death assemblage as a recorder of climate change and the reorganization of the continental shelf benthos. Palaeogeogr. Palaeoclimatol. Palaeoecol. **537**: 109205. doi:10.1016/j.palaeo.2019.05.027.

Powell, E.N., Gendek, J.J., and Ashton-Alcox, K.A. 2005. Fisherman choice and incidental catch: size frequency of oyster landings in the New Jersey oyster fishery. J. Shellfish Res. **24**: 469–476. doi:10.2983/0730-8000(2005)24[469:FCAICS]2.0.CO;2.

Powell, E.N., Hofmann, E.E., Klinck, J.M., and Ray, S.M. 1992. Modeling oyster populations I. A commentary on filtration rate. Is faster always better? J. Shellfish Res. **11**: 387–398.

Powell, E.N., Klinck, J.M., Hofmann, E.E., and Ray, S.M. 1994. Modeling oyster populations. IV: rates of mortality, population crashes and management. Fish. Bull. **92**: 347–373.

Powell, E.N., Klinck, J.M., Hofmann, E.E., Wilson-Ormond, E.A., and Ellis, M.S. 1995. Modeling oyster populations. V. Declining phytoplankton stocks and the population dynamics of American oyster (*Crassostrea virginica*) populations. Fish. Res. **24**: 199–222. doi:10.1016/0165-7836(95)00370-P.

Powell, E.N., Kreeger, D.A., Morson, J.M., Haidvogel, D.B., Wang, Z., Thomas, R., and Gius, J.E. 2012. Oyster food supply in Delaware Bay: estimation from a hydrodynamic model and interaction with the oyster population. J. Mar. Res. **70**: 469–503. doi:10.1357/002224012802851904.

Powell, E.N., Trumble, J.M., Mann, R.L., Long, M.C., Pace, S.M., Timbs, J.R., and Kuykendall, K.M. 2020b. Growth and longevity in surfclams east of Nantucket: range expansion in response to the post-2000 warming of the North Atlantic. Cont. Shelf Res. **195**: 104059. doi:10.1016/j.csr.2020.104059.

Pütter, A. 1920. Studien über physiologische Ähnlichkeit VI. Wachstumsähnlichkeiten. Pflügers Archiv für die gesamte Physiologie des Menschen und der Tiere, **180**: 298–340.

Queiros, Q., McKenzie, D.J., Dutto, G., Killen, S., Saraux, C., and Schull, Q. 2024. Fish shrinking, energy balance and climate change. Sci. Total Environ. **906**: 167310. doi:10.1016/j.scitotenv.2023.167310.

Quijón, P.A., Grassle, J.P., and Rosario, J.M. 2007. Naticid snail predation on early post-settlement surfclams (*Spisula solidissima*) on the inner continental shelf of New Jersey, USA. Mar. Biol. **150**: 873–882. doi:10.1007/s00227-006-0399-9.

Rao, K.P. 1953. Rate of water propulsion in *Mytilus californianus* as a function of latitude. Biol. Bull. **104**: 171–181. doi:10.2307/1538791.

Ray, C. 1960. The application of Bergmann's and Allen's Rules to the poikilotherms. J. Morphol. **106**: 85–108. doi:10.1002/jmor.1051060104.

Reimers, C.E., Taghon, G.L., Fuller, C.M., and Boehme, S.E. 2009. Seasonal patterns in permeable sediment and water-column biogeochemical properties on the inner shelf of the Middle Atlantic Bight. Deep-Sea Res. II Top. Stud. Oceanogr. **56**: 1865–1881. doi:10.1016/j.dsr2.2009.05.027.

Ren, J.S., and Ross, A.H. 2005. Environmental influence on mussel growth: a dynamic energy budget model and its application to the greenshell mussel *Perna canaliculus*. Ecol. Modell. **189**: 347–362. doi:10.1016/j.ecolmodel.2005.04.005.

Riisgård, H.U. 2001a. On measurement of filtration rates in bivalves——the stony road to reliable data: review and interpretation. Mar. Ecol. Prog. Ser. **211**: 275–291. doi:10.3354/meps211275.

Riisgård, H.U. 2001b. Physiological regulation versus autonomous filtration in filter-feeding bivalves: starting points for progress. Ophelia **54**: 193–209. doi:10.1080/00785236.2001.10409465.

Rio-Portilla, M.A. del, and Beaumont, A.R. 2001. Heterozygote deficiencies and genotype-dependent spawning time in *Mytilus edulis*. J. Shellfish Res. **20**: 1051–1057.

Ropes, J.W. 1968. Reproductive cycle of the surf clam, *Spisula solidissima*, in offshore New Jersey. Biol. Bull. **135**: 349–365.

Roy, K., Jablonski, D., and Valentine, J.W. 2001. Climate change, species range limits and body size in marine bivalves. Ecol. Lett. **4**: 366–370. doi:10.1046/j.1461-0248.2001.00236.x.

Rudders, D., Mann, R., Borsetti, S., Munroe, D., McCarty, A., Aponte, R., et al. 2024. Resource monitoring for Atlantic surfclam (*Spisula solidissima*) at the Coastal Virginia Offshore Wind development site. Virginia Institute of Marine Science Marine Resource Report, #2024-04, Virginia Institute of Marine Science, Gloucester Point, Virginia. doi:10.25773/dv7y-j464.

Saba, V. S., Griffies, S. M., Anderson, W. G., Winton, M., Alexander, M. A., Delworth, T. L., et al. 2016. Enhanced warming of the northwest Atlantic Ocean under climate change. J. Geophys. Res.: Oceans, **121**: 118–132. doi:10.1002/2015JC011346.

Sampognaro, L., and Segura, A. M. 2024. Biogeographic trends in populations of the shrimp *Artemesia longinaris* (Decapoda: Penaeidae) on the Atlantic coast of South America. Fish. Res. **272**: 106954. doi:10.1016/j.fishres.2024.106954.

Savage, N. B. 1976. Burrowing activity in *Mercenaria mercenaria* (L.) and *Spisula solidissima* (Dillwyn) as a function of temperature and dissolved oxygen. Mar. Behav. Physiol. **3**: 221–234. doi:10.1080/10236247609378513.

Scheld, A. M., Beckensteiner, J., Munroe, D. M., Powell, E. N., Borsetti, S., Hofmann, E. E., and Klinck, J. M. 2022. The Atlantic surfclam fishery and offshore wind energy development: 2. Assessing economic impacts. ICES J. Mar. Sci. **79**: 1801–1814. doi:10.1093/icesjms/fsac109.

Schöne, B. R., Houk, S. D., Freyre Castro, A. D., Fiebig, J., Oschmann, W., Kröncke, I., et al. 2005. Daily growth rates in shells of *Arctica islandica*: assessing sub-seasonal environmental controls on a long-lived bivalve mollusk. Palaios, **20**: 78–92. doi:10.2110/palo.2003.p03-101.

Selin, N. I. 2010. The growth and life span of bivalve mollusks at the northeastern coast of Sakhalin Island. Russ. J. Mar. Biol. **36**: 258–269. doi:10.1134/S1063074010040048.

Serna-Gallo, I., Ruiz-Valazco, J. M. J., Acosta-Salmón, H., Peña-Massina, E., Torres-Zepeda, G., and Saucedo, P. H. 2014. Growth and reproduction patterns of the winged pearl oyster, *Pteria sterna*, cultivated in tropical environments of Mexico: implications for pearl farming. Cienc. Mar. **40**: 75–88. doi:10.7773/cm.v40i2.2393.

Shumway, S. E., Sherman, S. A., Cembella, A. D., and Selvin, R. 1994. Accumulation of paralytic shellfish toxins by surfclams, *Spisula solidissima* (Dillwyn, 1897) in the Gulf of Maine: seasonal changes, distribution between tissues, and notes on feeding habits. Nat. Toxins, **2**: 236–251. doi:10.1002/nt.2620020413.

Sirén, A. P. K., and Morelli, T. L. 2020. Interactive-range-limit theory (iRLT): an extension for predicting range shifts. J. Anim. Ecol. **89**: 940–954. doi:10.1111/1365-2656.13150.

Smith, E. B., Williams, F. M., and Fisher, C. R. 1997. Effects of intrapopulation variability on von Bertalanffy growth parameter estimates from equal mark-recapture intervals. Can. J. Fish. Aquat. Sci. **54**: 2025–2032. doi:10.1139/f97-110.

Spencer, M. M., Powell, E. N., Klinck, J. M., Munroe, D. M., LeClaire, A. M., Borsetti, S., et al., in press. Climate-induced warming on the Mid-Atlantic Bight continental shelf: predictions of the future distribution and carrying capacity of the Atlantic surfclam (*Spisula solidissima*) and the expanding ecotone with the ocean quahog (*Arctica islandica*). Fish. Oceanogr. doi:10.1111/fog.12709.

Stauber, L. A. 1950. The problem of physiological species with special reference to oysters and oyster drills. Ecology, **31**: 109–118. doi:10.2307/1931365.

Stromp, S. L., Powell, E. N., and Mann, R. 2023. Evaluation of the degree of co-occurrence of Atlantic surfclams (*Spisula solidissima*) and ocean quahogs (*Arctica islandica*) in the expanding northwestern Atlantic boreal/temperate ecotone: implications for their fisheries. J. Shellfish Res. **42**: 61–75. doi:10.2983/035.042.0107.

Talevi, J., Steeves, L., Coffin, M., Guyondet, T., Sakamaki, T., Comeau, I., and Filguetra, R. 2023. The physiological state of four commercially important bivalve species during a naturally occurring heatwave. Can. J. Zool. **101**: 913–929. doi:10.1139/cjz-2022-0215.

Then, A. Y., Hoenig, J. M., Gedamke, T., and Ault, J. S. 2015. Comparison of two length-based estimators of total mortality: a simulation approach. Trans. Am. Fish. Soc. **144**: 1206–1219. doi:10.1080/00028487.2015.1077158.

Timbs, J. R., Powell, E. N., and Mann, R. 2018. Assessment of the relationship of stock and recruitment in the Atlantic surfclam *Spisula solidissima* in the northwestern Atlantic Ocean. J. Shellfish Res. **37**: 965–978. doi:10.2983/035.037.0507.

Timbs, J. R., Powell, E. N., and Mann, R. 2019. Changes in the spatial distribution and anatomy of a range shift for the Atlantic surfclam *Spisula solidissima* in the Mid-Atlantic Bight and on Georges Bank. Mar. Ecol. Prog. Ser. **620**: 77–97. doi:10.3354/meps12964.

Ulrich, P. N., and Marsh, A. G. 2008. Proteome assay of temperature stress and protein stability in extreme environments: groundwork with the heat stress response of the bivalve *Mercenaria mercenaria*. J. Shellfish Res. **27**: 241–246. doi:10.2983/0730-8000(2008)27[241:PAOTSA]2.0.CO;2.

Vakily, J.M. 1992. Determination and comparison of bivalve growth, with emphasis on Thailand and other tropical areas. ICLARM Tech. Rpt. **36**: 125.

van der Veer, H. W., Cardoso, J. F. M. F., and van der Meer, J. 2006. The estimation of DEB parameters for various northeast Atlantic bivalve species. J. Sea Res. **56**: 107–124. doi:10.1016/j.seares.2006.03.005.

Van Wynsberge, S., Andréfouët, S., Gilbert, A., Stein, A., and Remoissenet, G. 2013. Best management strategies for sustainable giant clam fishery in French Polynesia Islands: answers from a spatial modeling approach. PLoS One, **8**(5): p. e64641. doi:10.1371/journal.pone.0064641.

Verberk, W. C. E. P., Atkinson, D., Hoefnagel, K. N., Hirst, A. G., Horne, C. R., and Siepel, H. 2021. Shrinking body sizes in response to warming: explanations for the temperature-size rule with special emphasis on the role of oxygen. Biol. Rev. **96**: 247–268. doi:10.1111/brv.12653.

Von Bertalanffy, L. 1938. A quantitative theory of organic growth (inquiries on growth laws. II.). Hum. Biol. **10**: 181–213.

Wagner, T., Schliep, E. M., North, J. S., Kundel, H., Custer, C. A., Ruzich, J. K., and Hansen, G. J. A. 2023. Predicting climate change impacts on poikilotherms using physiologically guided species abundance models. Proc. Natl. Acad. Sci. **120**: e2214199120. doi:10.1073/pnas.2214199120.

Watanabe, S., Katayama, S., Kodama, M., Cho, N., Nakata, K., and Fukuda, M. 2009. Small-scale variation in feeding environments for the Manila clam *Ruditapes philippinarum* in a tidal flat in Tokyo Bay. Fish. Sci. **75**: 937–945. doi:10.1007/s12562-009-0113-1.

Weinberg, J. R. 2005. Bathymetric shift in the distribution of Atlantic surf-clams: response to warmer ocean temperatures. ICES J. Mar. Sci. **62**: 1444–1453. doi:10.1016/j.icesjms.2005.04.020.

Weinberg, J.R. 1998. Density-dependent growth in the Atlantic surfclam, *Spisula solidissima*, off the coast of the Delmarva Peninsula, USA. Mar. Biol. **130**: 621–630. doi:10.1007/s002270050284.

Weinberg, J.R., Powell, E.N., Pickett, C., Nordahl, V.A., Jr., and Jacobson, L.D. 2005. Results from the 2004 cooperative survey of Atlantic surfclams. Northeast Fish. Sci. Cent. Ref. Doc. **05–01**: 1–41.

Weymouth, F. W., McMillin, H. G., and Rich, W. H. 1931. Latitude and relative growth in the razor clam, *Siliqua patula*. J. Exp. Biol. **8**: 228–249. doi:10.1242/jeb.8.3.228.

Wilkin, J., Levin, J., Moore, S., Arango, H., López, S., and Hunter, E. 2022. A data-assimilative model reanalysis of the U.S. Mid Atlantic Bight and Gulf of Maine: configuration and comparison to observations and global ocean models. Prog. Oceanogr. **209**: 102919. doi:10.1016/j.pocean.2022.102919.

Williams, G. H., and Blood, C. L. 2003. Active and passive management of the recreational fishery for Pacific halibut off the U.S. west coast. N. Am. J. Fish. Manag. **23**: 1359–1368. doi:10.1577/M01-233AM.

Wisner, B., Wang, Z., Sheehan, A., Guo, X., and Munroe, D. 2024. Genetics, age demographics, and shell size of Atlantic surfclams from the southern edge of their range. Estuaries Coasts, **47**: 485–493. doi:10.1007/s12237-023-01281-z.

Woodin, S. A., Hilbish, T. J., Helmuth, B., Jones, S. J., and Wethey, D. W. 2013. Climate change, species distribution models, and physiological performance metrics: predicting when biogeographic models are likely to fail. Ecol. Evol. **3**: 3334–3346. doi:10.1002/ece3.680.

Xu, Y., Miles, T., and Schofield, O. 2020. Physical processes controlling chlorophyll-a variability on the Mid-Atlantic Bight along northeast United States. J. Mar. Syst. **212**: 103433. doi:10.1016/j.jmarsys.2020.103433.

Yoder, J. A., Schollaert, S. E., and O'Reilly, J. E. 2002. Climatological phytoplankton chlorophyll and sea surface temperature patterns in continental shelf and slope water off the northeast U.S. coast. Limnol. Oceanogr. **47**: 672–682. doi:10.4319/lo.2002.47.3.0672.

Yu, Z., and Guo, X. 2006. Identification and mapping of disease-resistance QTLs in the eastern oyster, *Crassostrea virginica* Gmelin. Aquaculture, **254**: 160–170. doi:10.1016/j.aquaculture.2005.10.016.

Zang, Z., Ji, R., Feng, Z., Chen, C., Li, S., and Davis, C. S. 2021. Spatially varying phytoplankton seasonality on the Northwest Atlantic shelf: a model-based assessment of patterns, drivers, and implications. ICES J. Mar. Sci. **78**: 1920–1934. doi:10.1093/icesjms/fsab102.

Zang, Z., Ji, R., Hart, D. R., Chen, C., Zhao, L., and Davis, C. S. 2022. Modeling Atlantic sea scallop (*Placopecten magellanicus*) scope for growth on the northeast U.S. shelf. Fish. Oceanogr. **31**: 271–290. doi:10.1111/fog.12577.

Zang, Z., Ji, R., Hart, D. R., Jin, D., Chen, C., Liu, Y., and Davis, C. S. 2023. Effects of warming and fishing on Atlantic sea scallop (*Placopecten magellanicus*) size structure in the Mid-Atlantic rotationally closed area. ICES J. Mar. Sci. **80**: 1351–1366. doi:10.1093/icesjms/fsad063.

Zhang, X., Haidvogel, D., Munroe, D., Powell, E. N., Klinck, J., Mann, R., and Castruccio, F. S. 2015. Modeling larval connectivity of the Atlantic surfclams within the Middle Atlantic Bight: model development, larval dispersal and metapopulation connectivity. Estuarine Coastal Shelf Sci. **153**: 38–53. doi:10.1016/j.ecss.2014.11.033.

Zhang, X., Munroe, D., Haidvogel, D., and Powell, E. N. 2016. Atlantic surfclam connectivity within the Middle Atlantic Bight: mechanisms underlying variation in larval transport and settlement. Estuarine Coastal Shelf Sci. **173**: 65–78. doi:10.1016/j.ecss.2016.02.019.

Zuo, W., Moses, M. E., West, G. B., Hou, C., and Brown, J. H. 2012. A general model for effects of temperature on ectotherm ontogenetic growth and development. Proc. R Soc. B Biol. Sci. **279**: 1840–1846. doi:10.1098/rspb.2011.2000.